6-2-1997

Nitrogen Gas Generation and Diffusion from Diazo Reproducution Materials

David R. Anderson

NITROGEN GAS GENERATION AND DIFFUSION FROM DIAZO REPRODUCTION MATERIALS.

PRESENTED IN PARTIAL FULFILLMENT OF A
MASTERS DEGREE IN PHOTOGRAPHIC SCIENCE,
ROCHESTER INSTITUTE OF TECHNOLOGY

2 June 1977

BY: David R. Anderson

ABSTRACT

It has been hypothesised that generation of nitrogen during exposure by diazo duplication materials can contribute to image degradations in microform and aerial negative reproductions. Research was conducted to investigate the rate generated gas is diffused from the surface and possible film-film separations this gas may cause during contact printing. Apparatus was constructed to measure gas diffusion rates and simulated film-film separations during exposure. Diffused gas was collected in a rubber diaphragm whose expansion was measured using a variable capacitor tuned oscillator technique. To simulate printer film-film separations movement of a 5.4 x 7.5 cm. glass plate placed on the film was measured during exposure. A metal-halide mercury vapor lamp and optical system in the apparatus projected sufficient energy to destroy one half the potential density in 2.4 to 5.7 seconds. This time depended upon the type of film used. Measured gas diffusion rates ranged from 3.3×10^{-10} to 9.2×10^{-9} mole/sq cm/sec for the four positive working diazo films evaluated. Plate-film separations up to 2.2 um were measured. It was also determined that gas release is not instantaneous upon exposure and that gas continues to be diffused after exposure has terminated. In addition exposures from the top and bottom of the emulsion produce different initial gas release rates. Analytical models were developed to correlate experimental data with printer film-film separations. Measured plate-film separations were less than predicted by the models. It is believed that the models are correct and that during the plate-film separation experiments the film had an initial curl, thus violating the parallel initial zero separation condition and explaining the differences.

I. INTRODUCTION:

Diazo photographic films are extensively used for microform reproductions and are being investigated for possible use in aerial imagery duplication. To accommodate large production rates, high intensity, high speed contact printers are required. Excellent image quality is not realized unless the original imagery and duplication material are held in register and contact during exposure. In the past, reproductions have not achieved anticipated results; image quality being less than desired. Film manufacturers have recognized that this problem could be caused by nitrogen generation within the film during exposure. It has been hypothisized that this nitrogen diffuses from the emulsion into the area between the original and duplication material causing a separation. Thus image quality is lost due to optical geometry, optical diffraction and/or mechanical slippage during printing. To combat this separation problem manufacturers have modified their films to reduce the rate nitrogen is expelled.[1/]

This phenomenon appears analogous to an air bearing where gas is injected between two surfaces to separate and lubricate. The higher the gas flow rate the greater the pressure causing this separation. Thus in diazo printing, for higher exposure rates, larger gas diffusion rates would be expected, and in turn greater original-duplicate separations. In recent Air Force tests of a high speed aerial film contact printer an exposure rate image quality dependency was experienced; transfer resolution being better at lower than higher printing rates.[2/] The cause of this dependency has not been determined but the effect correlates with the gas diffusion air bearing idea.

Gas diffusion rates have not previously been determined for diazo films. Also the amount of film separation that this gas could cause has not been measured. This was the purpose of the research. Apparatus was designed and constructed to measure the rate of nitrogen diffusion during exposure. Also the movement of a glass plate placed on top of the film was measured. This was an attempt to simulate original-duplicate separation during printing. An analytical expression was also derived to correlate gas diffusion rate with anticipated diazo duplication material-original film separation. Attempts to match this expression with measured plate-film separations were marginally successful.

The theory/logic behind the experiments, the apparatus design, the experimental procedures and the results will be discussed. No attempt was made to determine if the gas generated was nitrogen. Also no correlation of gas generation rate with anticipated image quality of reproductions was made; significance of the rates found was not determined. The gas diffusion rates and plate separations measured in no way imply quality of the diazo products used in these experiments. These image quality questions are subjects for further investigations.

II. THEORY:

A. Diazo Materials:

1. Nitrogen gas is a by product of the conventional positive working diazo photo decomposition reaction. During exposure a diazo molecule absorbs a photon causing its decomposition. Of the many possible reaction by products nitrogen molecules (N_2) are included. Nitrogen being non-reactive will stay in gaseous form and migrate out of the emulsion. Along with diazo molecules the normally acidic emulsions contain couplers which in an alkaline environment react with the diazo molecules to form azo dyes. After exposure the film is subjected to an ammonia atmosphere, thus making the emulsion basic and causing development.
2. Using information available in Dinaburg's book on diazo compounds [3] it was estimated that diazo concentrations in the order of 10^{-8} to 10^{-7} moles/sq cm could be anticipated. During a printing exposure it is assumed that one half the molecules are decomposed. For high speed printing, exposure times of one second have been used. Thus gas generation rates of 5×10^{-8} moles/sq cm/sec could be anticipated. The question here concerns the rate gas is expelled from the emulsion; the gas diffusion rate. This rate will determine film separation during exposure.

3. Negative working diazo materials do not operate on this principle. One published process used the photo decomposition of a diazosulfonate molecule to a diazo compound. The diazosulfonate will not couple but the diazo compound will.[4/]

B. The separation of two plain parallel plates due to a gas flow can be explained using fluid dynamics theory. Employing a few assumptions, equations were developed describing separation during exposure for films in the experimental apparatus and for a roll to roll contact printer.

1. Assumptions were used to simplify the mathematics. The first of these were that the gas flow is laminar, the only restricting force viscous and that the gas is non-compressible. Secondly it was assumed that gas is generated uniformly across the surface of the film. For the plate film separation experiment it was assumed that a circular disk of equivalent area approximates the rectangular plate situation. And lastly to describe a contact printer separation it was assumed that gas flows only perpendicular to the length of film; toward the edges. The first simplifications are good with the only exception being that at very small separations the flow may be molecular and not laminar. Pressures are too small, much less then one atmosphere, to significantly compress the gas. Gas generation should be uniform in the experimental apparatus but for a duplication printer the gas is generated at a rate inversly proportional to the density of the original at that area. However, the uniform gas generation assumption should be reasonable considering the varying densities over a large area.

2. Derivation: Experimental plate film separation; (6)

a. Consider two parallel disks separated a distance a. The velocity of a fully developed laminar gas flow can be described by the following clasic equation.

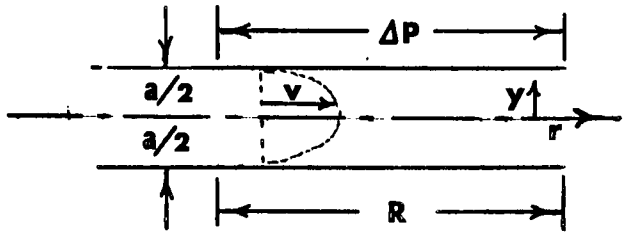

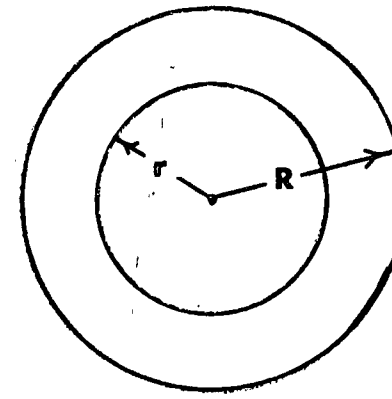

$$v_r = \frac{dP}{2\mu\, dr}\left(y^2 - \frac{a^2}{4}\right)$$

Flow rate equals:

$$dQ_r = v_r\, dA = v_r\, 2\pi r\, dy$$

$$\int_0^{Q_r} dQ_r = \int_{a/2}^{a/2} \frac{\pi r\, dP}{\mu\, dr}\left[y^2 \frac{a^2}{4}\right] dy$$

$$Q_r = \frac{\pi r a^3}{6\mu}\frac{dP}{dr}$$

Consider that the gas flowing from between the two plates receives equal contributions from all areas of the disk. This is logical because the gas generation rate has been assumed constant and the gas is non-compressable. As will be discussed later, gas not participating in the flow will accumulate causing plate-film separation. This gas flow contribution rate per unit area is Q.

WHERE: $Qr = Q'\pi r$

$$\int_e^{\Delta P} dp = \int_o^R (6\mu Q'/a^3)\, rdr$$

$$\Delta P = 3\mu Q' R^2 / a^3$$

$$\Delta P = (3\mu Q'\pi R^2)/(\pi a^3) = (3\mu Q' A)/(\pi a^3)$$

For the rectangle approximation: $A = LW$

Therefore $Q' = (\pi a^3 \Delta P)/(3\mu LW)$

And $Q = Q'LW = (\pi a^3 \Delta P)/(3\mu)$

3. For a dynamic situation the plate and film start together, i.e. a = o, therefore, the flow rate from between the two surfaces is also zero. Gas is generated uniformly at a rate F due to decomposition of diazo molecules. Before being expelled the gas collects between the two plates separating them. As the separation increases so does the expelled flow rate until the gas generation rate and expelled flow rates are equal.

   The rate at which the volume of trapped gas is changing at any instant in time is the difference between the gas generated and the gas expelled. At steady state no further change occurs to the volume of trapped gas.

$$V_t = \sum_{n=1}^{k+1} \left[FLW - Q_{(a)} \right] \Delta t; \quad t = K\Delta t$$

Plate separation is: $a = V/LW$

$$a_t = \sum_{n=1}^{k+1} \left[22.4 \times 10^3 R - \frac{\pi \Delta P}{3\mu LW} (a_{n-1})^3 \right] \Delta t$$

NOTE: Assuming near standard-temperature-pressure conditions.

WHERE: R = gas diffusion rate (mole/sq cm/sec)

μ = viscousity (dyne/cm/sec)

P = pressure forcing two surfaces together (dynes/sq cm)

W = width of surfaces (cm)

L = length of surfaces (cm)

t = exposure time (sec)

AT THE LIMIT:

$$a = \left[\frac{3\mu LW\ (22.4 \times 10^3 R)}{\pi\ \Delta P} \right]^{1/3}$$

4. Derivation: Roll to roll contact printer;

(a) A conventional technique for roll film duplication is to bring two rolls of material, original and duplication product, over a drum. Exposing radiation strikes the materials over a portion of the contact area. Because of low sensitivity of diazo materials and high printing speed requirements the exposing surface may be several centimeters long. For narrow materials the length of the exposing surface may greatly exceed the width. Therefore, the gas flow would be perpendicular to the film path because it is the path of least resistance. For wider materials perpendicular flow is also anticipated but for a different reason. There is no exposure at the beginning and end of contact area. Therefore, the separation should approach zero and restrict flow in the lengthwise direction.

(b) Consider two parallel plates separated a distance a. with width W and length L.:

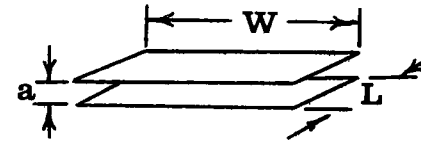

$$Vx = dp/(2\mu dx)\ (y^2 - a^2/4)$$

$$dQx = VxdA = vLdy$$

$$Qx = a^3 L/(12\mu)\ dp/dx$$

$$Qx = Q'LX$$

$$\int_0^{\Delta P} dp = \int_0^{W/2} \left(12\mu Q'/a^3\right) xdx$$

$$\Delta P = 3\mu Q' W^2/(2a^3)$$

$$Q = Q'LW = 2\Delta P a^3 L/(3\mu W)$$

As with the disk approximation of the rectangle derivation:

$$a_t = \sum_{n=1}^{K+1} \left[22.4 \times 10^3 R - 2\Delta P/(3\mu W^2)\ (a_{n-1})^3 \right] \Delta t;\ t = K\Delta t$$

at the limit

$$a = \left[3\mu W^2\ (22.4 \times 10^3 R)/(2\Delta P) \right]^{1/3}$$

5. The critical relationship in these equations is the separation cubed dependency. The disk model for rectangular flow and the perpendicular flow for contact printer assumptions do not affect this dependency. They only change less significant constants. The equations are not exact models of situations depicted but are very good representations. In Section IV and V the relationship of these equations with experimental data will be discussed.

C. Method of analysis: From the other theory discussions we could anticipate gas generations of up to 5×10^{-8} moles/sq cm and film separations of a few micrometers. The question is how to measure with any degree of accuracy these very small quantities and distances.

1. Several techniques were tried with little success to detect loss of nitrogen by exposure.

   (a) First attempts were weighing experiments. That is weighing a quantity of film (1.0 sq m) on an analytical balance. Then exposing the film and reweighing it. The difference should be the loss in nitrogen. Losses of up to (5×10^{-8} mole/sq cm $\times 10^4$ sq cm/sq m $\times$ 28 gr/mole) = 0.014 grams could be expected. Using P4-150 film variances in weight were found, however, they greatly depended upon room humidity, i.e. moisture content of the film. Attempts were made to stabilize the film by heating it in an oven before each weighing. This proved moderately successful. It must be kept in mind that there is no guarantee that the susceptibility to moisture is the same for exposed and non-exposed film. For example HCl is a by-product of some diazo decomposition reactions and it has an affinity for water.

(b) Also tried was viewing gas bubbles formed in a layer of oil placed on the surface during exposure. None were detected. Another direct measurement involved a simple water filled u-tube manometer placed over the film during exposure. A rubber gasket at the bottom of the manometer retained any released gas. No pressure changes were seen that could be attributed to diffused gas. These experiments were only made with the Scott Graphics P4-150 film, a film later found to have a low gas diffusion rate. These simple techniques may work well with other diazo materials.

2. The techniques used to measure film separations and gas rate discharge employed a capacitor tuned oscillator and a rubber diaphragm. Small movements were transferred to a parallel plate capacitor, closing the plates. This in turn lowered the frequency of the tuned oscillator. These movements were either separation of a plate and film or the expansion of the rubber diaphragm as it collects gas.

(a) The capacitance of a parallel plate capacitor in air is given by:

$$C_t = \frac{8.85 \times 10^{-14} A}{d}$$

WHERE: A = area of one plate (sq cm)

d = separation (cm)

C_t = capacitance (farads)

The capacitance of the tuning network of an oscillator is equal to the capacitance of test capacitor C_t and the internal oscillator capacitance C_i. : $C = C_i + C_t$

The frequncy of oscillation is:

$$f = \frac{1}{2\pi\sqrt{LC}} \quad , \quad L = 1/(4\pi^2 f^2 C)$$

WHERE: f = frequency (Hertz)

L = Inductance (Henry)

OR: $C = \frac{1}{4\pi^2 f^2 L} = C_i = C_t$

$$\frac{8.5 \times 10^{-14} A}{d} = \frac{1}{4\pi^2 f^2 L} - C_i = \frac{1 - 4\pi^2 f^2 L C_i}{4\pi^2 f^2 L}$$

$$d = \frac{8.5 \times 10^{-14} A \, 4\pi^2 f^2 L}{1 - 4\pi^2 f^2 L C_i}$$

$$d_1 - d_2 = \Delta d = 3.36 \times 10^{-12} AL \left[\frac{f_1^2}{1 - 39.5 f_1^2 L C_i} - \frac{f_2^2}{1 - 39.5 f_2^2 L C_i} \right]$$

Consider the case where f_1 = 9.9 MHz, d = 0.025 cm,

C_i = 150 uuf. and, A = 7.07 cm^2

THEN: C_t = 25.0 uuf

L = 1.48 uh

Relatively non-complex equipment can easily measure a 100 Hz change in frequency. For a 100 Hz change f_2 = 9.8999 MHz. For this frequency change d = 3.52×10^{-6} cm = 0.035 um. Clearly this capacitor-oscillator technique provides a very sensitive movement detection device.

(b) The technique used for measuring gas discharge rate involved collecting the gas during exposure in a rubber diaphragm. The diaphragm expands into a spherical segment. Volume of gas will be directly proportional to the height of the segment. This height is measured using the capacitor tuned oscillator technique.

The volume of a spherical segment = $V = 1/6\ h\ (h^2-3a^2)$

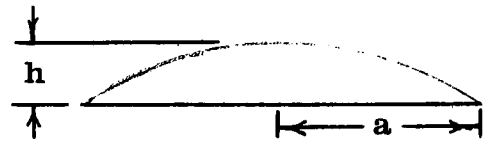

If $a \gg h$ then: $V \simeq 1/2\,\pi h a^2$

Volume/unit area - $V/A = (1/2\,\pi h a^2)/\pi a^2 = h/2$

From the general gas equation $PV = nrt$

$n/A = hP/(2rt)$

for P = 1 atm, T - 300 K

$n/A = 2.03 \times 10^{-9}$ h (um) mole/cm^2

Then gas diffusion rate is: $R = \frac{d\ (n/A)}{dt} \simeq \frac{n/A}{T}$

All that needs to be determined is the height of the spherical segment. Anticipated maximum values of "h" based on estimates of nitrogen generated is about 20 um. However, to measure a gas diffusion rate the value of h must be measured several times during exposure. Thus the equipment must be capable of measuring much less than 20 um, approximately 1 um. To measure one micrometer the accuracy of the device should be an order of magnitude better, i.e. .1 um. A goal easily met by the capacitor-oscillator technique.

III. TEST APPARATUS (Figure 1):

The requirements for the test apparatus were to rapidly expose diazo materials and during the exposure measure gas generated or movement in a glass plate placed over the diazo film. This required producing a high power source of near ultraviolet radiation concentrated on a film plane. Also it meant devising a method of trapping and measuring small quantities of gas. Lastly very small changes in separation, distances less than 0.1 um had to be measured. These were very stringent requirements for a student constructed apparatus. Four months were spent designing and testing this apparatus prior to conducting actual experiments. First the construction of the equipment will be reviewed then its calibration discussed.

A. Description of Apparatus: The apparatus consists of an illumination system, a variable capacitor and electronic support equipment.

1. Illumination System (Figure 2): Diazo films are sensitive to the near ultraviolet portion of the spectrum. The effective range for one film used, Scott Graphics P4-150, is approximately 375 to 475 nm[5/]. Also sufficient intensity was desired so that during a one second exposure one half the available diazo molecules would be destroyed, (a requirement that was not met). The system choice was a mercury vapor lamp focused onto an illumination plane using a condenser lens. A 45 degree mirror was included to permit a horizontal film plane, and a shutter added to regulate exposure time. The system is housed in two mechanically isolated boxes. Precautions were taken to prevent mechanical vibration from interfering with test measurements.

   (a) Source: A GTE Sylvania 400 watt Metalarc 46, M400BD lamp was chosen as the source of illumination. It is mounted vertically, base down in a porcelain socket and powered by a Jefferson Electronic N.I.O. lamp ballast 855-1330 type CWA. This is a metal halide mercury vapor lamp. During experiments this lamp and a conventional mercury vapor lamp, H400A33-1/T16, were evaluated, the "effective" radiance of the mercury lamp was approximately one half that of the metal halide lamp (see table 1a).

   (b) Condenser: The radiant energy from the lamp was focused onto the film plane by two 11.3 cm diameter, 16.5 cm focal length, plano-convex condenser lenses. The lamp image distances, (approximately 11 and 33 cm) were adjusted so that the lamp arc was focused onto the film plane with a magnification of three. This allowed coverage of the 4.5 x 10 cm film plane with a 1.5 cm x 4.7 cm lamp arc. The irradiance of the film plane was not uniform; this is primarily because the energy within the lamp's arc is concentrated at the center.

(c) Shutter (Figure 3): Exposure times were controlled by a shutter placed in the optical system between the lamp and condenser. The back plate was constructed of 1/8 in. composition board, the rails of 1/8 in. x 1 in. aluminum strips, and the blade of .030 in. aluminum sheet. Rubber bands provided the closing force for the blades which were released by magnetic latches. The shutter was cocked manually then the lower latch activated to expose the shutter opening and the upper latch activated to close the opening. The shutter opening is 3.5 in. x 4.5 in. cm, a size large enough to prevent vignetting. The shutter was placed between the lens and lamp so that during non-exposure time the condenser lens is not subjected to the heat generated by the lamp. This made an IR absorbing glass to protect the lens unnecessary. IR absorbing glass absorbs in the ultroviolet as well as infrared portion of the spectrum.

(d) Housing: The illumination system was incorporated into two mechanically isolated boxes (lamp and film plane) each constructed of 3/4 in. fir plywood. In addition to the lamp, ballast, shutter and condenser system the lamp box contained an exhaust blower for cooling. The film plane box contains the 45 degree mirror and supports for the capacitor-oscillator assembly. The two boxes are mechanically separated to prevent shutter and blower vibration from being transferred to the capacitor assembly. A circular 6 in. diameter hole in each box permits the transfer of radiant energy.

(e) Isolation: To prevent mechanical vibrations from interfering with capacitor-oscillators ability to measure minute movements both boxes were mounted on isolation platforms. The lamp box was set on three tennis balls placed in a triangular arrangement. This was to reduce

the transmission of shutter and blower vibrations through the floor and into the image plane box. Isolation for the image plane box consists of three 15 in. x 7.5 in. x 2.5 in. concrete patio stones placed on top of a one foot stack of newspapers. Both boxes were placed on a ground level concrete floor.

2. Capacitor-Oscillator Assembly (Figure 4): The capacitor system is a variable parallel plate capacitor with a nominal capacitance of 25 uuf. It is constructed to accommodate experiments of varying height and, with accessories, to measure both very small changes in distance and gas accumulations. The photographs show the construction and critical dimensions. This was the second unit constructed. The first was made of wood rather than aluminum and brass and did not have sufficient stability. Also it was very susceptible to humidity fluxuations.

   (a) Capacitor Plates: The upper capacitor is constructed of a 4 cm diameter mirror covered on one side with aluminum foil, the capacitor plate conducting surface. To attach the foil, lacquer was spread on the mirror and the foil pressed on with a piece of window glass, thus keeping it flat. An internally threaded brass bushing glued to the plate was used to attach it to the fine adjustment screw. The lower plate is a 3 cm diameter disk made of 1.6 mm thick copper clad phenolic printed circuit board stock. The disk is glued to the 3/16 in. diameter brass transfer tube. The effective plate size of the parallel plate capacitor is that of the smaller (lower) plate, 7.07 sq cm.

   (b) Lower Capacitor Plate Assembly: This assembly is composed of the lower capacitor plate, transfer tube, sensing disk and flexture bearings. A 2 cm diameter 1 mm thick glass disk is glued to the end of the transfer tube. This assembly is held parallel and allowed to move with two flexture type bearings. These essentially frictionless bearings were made from acetate film base material. Thus vertical movements of the sensing disk are transfered to the capacitor plate.

(c) Capacitor-Flexture-Adjustment Assembly: This assembly contains the capacitor plates, fine adjustments mechanism, and lower capacitor plate assembly. All mechanisms are attached to a slider which moves up and down along two guide rods, a screw (course adjustment) mechanism regulates this movement. This course adjustment allows the capacitor-flexture-adjustment assembly to be set for experiments of varying thicknesses. The idea is to have no bend in the flexturebearings at the onset of the experiment. As can be seen in the photographs shaped wire restrainers were added to the flexture bearings to reduce lateral bending.

(d) Support Structure: Constructed primarily of aluminum this structure provided the support for the capacitor-flexture-adjustment assembly, the 10.8 x 5.2 x .74 cm film plane glass, and oscillator electronics. The essential requirements were for this structure to be rigid and to maintain the sensing disk parallel to the image plane glass. This was accomplished by gluing the disk to the transfer tube after assembling the system. The support structure is held together by screws.

(e) Gas Collecting Apparatus: This is composed of a rubber membrane streatched over a 3.8 cm O.D. .2 cm thick plastic tube. The membrane is held in place by a 3.8 cm rubber gasket. The tube is 9.8 cm long and glued to a 5 cm x 7.5 cm x 3.2 mm plastic plate. A 2.6 cm hole is drilled in the plastic to accommodate the sensing probe. During experiments a gas seal is maintained by putting grease (Vaseline Petroleum Jelly) on the edges of the rubber diaphragm and holding the apparatus in place with two 140 gram lead weights. The apparatus is placed directly onto the emulsion side of the diazo film.

3. Electronics Assembly (Figure 5): This assembly provides shutter timing, measures the frequency of the oscillator/variable test capacitor and records frequency readings at specific time intervals during a test.

   (a) Timer: The shutter timing function provides pulses to the shutter assembly magnetic latches to activate the shutter blades. Timing can range from 0.1 sec to 10 sec in 0.1 sec intervals. The timer can also trigger the frequency monitoring device at either the beginning or end of shutter cycle. Shutter timing is required in experiments to determine exposure vs. density values for the various diazo films. It is also used in gas discharge experiments where the exposure is terminated prior to the end of the measuring experiment. For other experiments the shutter timer is used only to open the shutter and activate the frequency measuring device.

   (b) Oscillator: This is a colpitts type designed to operate in the 10 MHz range. The LC network that controls the operating frequency contains the variable test capacitor. As the capacitor plate separation increases the operating frequency lowers. Specifics of the electronic assembly are discussed in the attachment.

   (c) Frequency Monitoring Device: This is a digital frequency counter, a device that counts voltage pulses over a specific sample time and displays that count on a six digit readout. The sample times are 1 sec, .1 sec, and .01 sec. with a cutoff frequency of about 15 MHz.

   (d) Memory: To monitor plate separation changes during an experiment a memory circuit records up to 31 frequency readings 1 sec, .2 sec or .1 sec intervals depending upon the sample time used. These stored readings can be redisplayed at a later time for recording into a notebook. For the majority of my experiments the .1 sec sample time was used. This recorded a frequency measurement every 0.2 sec. Thus, frequency changes of the capacitor-oscillator for 6 seconds could be monitored. Later the frequency changes could be equated to changes in capacitor separation.

B. Calibration of Apparatus: Illumination system calibration consisted of finding the relative half density points of the diazo films used and of calibrating the Wratten neutral density filters used to control film plane irradiance. The capacitor-oscillator assembly was evaluated theoretically to determine its probable accuracy. The electronic assembly crystal controlled time base was adjusted against the WWV frequency standard.

1. Illumination System:

(a) Relative irradiance calibration consisted of producing exposure times vs. density curves for the diazo materials used in the experiments. The goal was to determine the exposure time required to destroy one half the available diazo molecules. This gives an indication of printing speed assuming that a photographic printing exposure would destroy one half the dye molecules. To accomplish this we assumed that the dye concentration is directly proportional to density (Beer's Law) and that the relative spectral density is unchanged with diffused density.

Three by twelve centimeter film samples were exposed for 0, 1, 2, 4, 6, 8, 10, 20 seconds and 5 minutes. The samples were processed using ammonia vapor. Two methods were used. The first was an Atlantic Blue-Ray, Model No. 609 Diazo Ammonia Vapor Processor. It used 28% Aquious Ammonia. Five passes were made through this small table top processor to ensure complete processing. The second method used aquious ammonia heated to 80 $\pm$ 2^{o}C in a 1.0 quart covered glass jar. The strips were suspended from the jar cover into the vapor for 1.5 minutes.

The density of the processed strips were determined using either a MacBeth TD504 or TD102 densitometer equipped with a visual filter. The center, lowest density, portion of the strip was evaluated. For evaluating diazo materials an infrared cutoff filter should be included in the densitometer as the azo dyes in the films have high infrared transmittance. Because the filter was not available the density values measured were not precise visual densities. The densities should be relative to film dye concentrations. A density vs. exposure time plot was generated for each film. From this, the exposure time correlating to one half density; $(D_o - (D_o - D_{5\ min.})/2)$; was found. This time correlates to the exposure required to destroy one half the diazo molecules. The results are shown in table 1a.

(b) Irradiance was controlled using Wratten 96 neutral density filters located at the illumination plane. As these filters do not have uniform spectral density they were calibrated for the diazo material used.

A time series was produced with 1, 2, 4, 6, 8, 10, 20 seconds and 5 minute exposures and ammonia vapor process. The densities were found and plotted against exposure time.

Then two strips of diazo film were exposed at 4.0 seconds using the neutral density filter to be calibrated. The strip was processed in ammonia vapor and the density determined. This average density was equated to an effective exposure time using the density time plot. Then assuming no reciprocity failure in diazo materials, the fractional change in irradiance caused by the neutral density filter is equal to the fractional change in effective time.

Effective Density = Log (effective time/4 seconds)

The results for GAF 2620P7 film are shown in table 1b.

(c) Comment: The goal was an illumination system with a one half density exposure of one second. This was to simulate high speed printing conditions. Preliminary calculation indicated that this was possible. These were based on the spectral distribution of a general electric metal halide lamp, the spectral sensitivity of scott graphics P4-150 film, the geometry of the optical system, and a rough guess at the absorption by the optical elements. What wasn't known is the actual energy distribution of the Sylvania lamp used, or the absorption of the glass in the optical system. As the lens and glasses were purchased surplus the type of glass was unknown. Other calibration areas were not considered. The variance in exposure over the image plane was evaluated only by general observation. Also irradiance of film plane and variations with time were not determined.

2. Electronics: The accuracy of the timer and frequency measuring functions is dependent upon switching time of the various electronic components and the accuracy of the crystal controlled time base. No attempt was made to evaluate switching times of electronic components. The crystal control oscillator of the time base was adjusted by beating the 1 MHz output with the WWV (10 MHz) carrier frequency. It is felt that the electronics is the most precise portion of the equipment; accuracy of data being limited by other areas, primarily the capacitor mechanical assemblies.

3. Capacitor-Oscillator Assembly: The calibration of the capacitor-oscillator is partially theoretical and partially experimental. The gas discharge and plate-film separation measurements are based on measuring changes in distance. These measurements as described in Section II are made by transfering these charges to the separation of a parallel plate capacitor. Capacitance

is based on theory which assumes a parallel condition. To predict the effect of the capacitor on the oscillator the inductance of the tuning coil and internal oscillator capacitance must be determined. An error is associated with this. These errors were determined and a worse case analysis made to evaluate the accuracy of the delta distance measurements.

(a) Capacitance: The capacitance of a parallel plate capacitor in air is given by C = 0.0885A/d. Where A is plate area and d the plate separation. This leads to a major possible area of error. That is the capacitor plates cannot be assumed parallel. Considering the size of the plates r = 1.5 cm and a nominal separation (d) of 0.25 mm for C = 25 uuf. Misalignment could not exceed 0.6 degrees or the plates would touch. Capacitance for a circular non-parallel plate capacitor can be described by:

$$C = \int_{-r}^{r} \frac{0.77\,(\,r^2 - x^2\,)^{\frac{1}{2}}}{d + X \tan\beta}\,dx$$

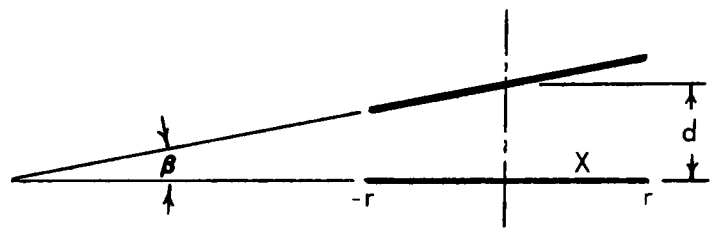

This inegral was solved numerically using an Hewlett Packard HP 9820A calculator. Capacitances for d = .2, .25, and .3 mm were evaluated for B angles of 0 and 0.6 degrees.

(b) Oscillator Calibration: The internal capacitance and inductance of the oscillator was determined by measuring the frequency of operation with no external capacitor,

with a pair of jumper wires, and with a 22 uuf $\pm$ 5% capacitor, attached with the jumper wires. With these three pieces of data the capacitance of the oscillator, and jumper wires and the inductance of the coil could be deduced.

$$\text{Frequency} = 1/(2\pi\sqrt{LC})$$

WHERE: L = inductance in henries

C = capacitance in farads

f = frequency in Hz

This equation was determined for three frequency capacitance sets: (C_1) internal capacitance; ($C_1 + C_2$) internal capacitance + wires; and ($C_1 + C_2 + C_3$) internal capacitance + wires + 22 uuf known capacitor. With this data L and C, could be calculated. The uncertainty concerning this calibration was knowledge of C_3, the known capacitor. It was a 22 uuf $\pm$ 5% ceramic capacitor. Considering the uncertainty the oscillator internal capacitance was found to be (156.4 uuf $<$ C $<$ 141.5 uuf) and the inductance (1.38 uh $<$ L $<$ 1.53 uh).

(c) Calculation of Oscillator-Capacitor Accuracy: Worst case conditions were evaluted to determine the maximum possible error in capacitor plate separation and changes in separation measurements. The worst case absolute distance measurement calibration curves are plotted in chart 1a, and the worst case delta distance curves in chart 1b. As can be seen, knowledge of plate separation is not good. However, over the area of interest f = 9.9 to 10.0 MHz knowledge at changes in separation is acceptable. Change in oscillator frequency vs. change in plate separation is:

(3530 Hz/ Δd(um) 4440)

Thus d = (3940 $\pm$ 13%) Hz, or knowledge of magnitude of Δd is within $\pm$ 13%.

It must be noted that this is not a variance. Even though the amount of error in d is not known it can be assumed to be fairly constant. The variables described should not change throughout the experiment. Actual variance was determined by replicating experiments.

4. Gas Collection Apparatus: As discussed in Section II the theoretical calibration of the apparatus is:

$$n/A = 2.03 \times 10^{-9} \text{ h (um)} \frac{\text{mole}}{\text{sq cm}}$$

This equation does not take into account any flattening of the diaphragm (from spherical) by the weight of the lower capacitor assembly. No attempt was made to approximate this effect. As the value of n/A is dependent upon h its accuracy is no better than $\pm$ 13%. Also the constant 2.03×10^{-9} is based on a temperature of 309K and pressure of 1 atm. A variance of 10^{o}C would cause a $\pm$ 3% variation in the measurement. As in the distance measuring evaluations variance was determined by replicating experiments.

IV. MATERIALS AND EXPERIMENTAL PROCEDURES:

A. Various aerial duplication and microform reproduction diazo films were used in these investigations. These included:

1. Scott Graphics Diazo P4-150: A special order positive working material used experimentally for aerial film reproductions.
2. Scott Graphics P4-900: A special order negative working material used experimentally for aerial film reproductions.
3. Keuffel and Esser (K&E) Positive Working: A special order positive working diazo material used experimentally for aerial film reproductions. Further nomenclature regarding this film was not available.
4. GAF 2620P7: A discontinued microform reproduction material.
5. Kodak Recordak Diazo M Film 4950: A microform reproduction material.

B. Experiments were conducted using these materials to investigate several factors regarding gas diffusion during exposure.

1. Determine the Gas Diffusion Rate During Constant Exposure: Using the diaphragm apparatus six measurements were made with the emulsion up, i.e. facing the rubber diaphragm. For each measurement the frequency counter time base was set at 0.1 sec and the readings recorded in the memory. The 31 frequency measurements were converted to moles/sq cm gas collected and plotted vs. time. The rate was determined from the straight line portion of this plot, normally between 2.0 and 5.0 seconds. The mean and variance of the six rates were calculated. Besides the expansion of the diaphragm due to collected gas, the capacitor plates could be compressed by thermal expansion of the apparatus caused by the exposing radiation. To determine this effect six base line measurements were made with the film emulsion side down. Any diffused gas would leak out and not expand the diaphragm. Movements were equated to effective gas discharge rates; mean and variance were found. It was assumed that the difference of these two means represent the actual discharge rate. To present the results, 95% confidence limits were placed on the difference of the two means. If zero was included in these limits than it was concluded that gas diffusion was not detected.
2. Determine If Gas Continues to Diffuse After Exposure: An emulsion up experiment was conducted as in part A except an exposure time of 3.0 seconds was used. Thus diffusion rate data collected included 3.0 seconds during exposure and 3.0 seconds after exposure. Gas quantity values were calculated and plotted vs. time. If no gas diffused after exposure terminated the rate, slope of graph, would go to zero.

3. Correlate Gas Diffusion Rate with Irradiance: Gas diffusion rates were determined as in part A for various film plane irradiances. Irradiance was controlled using calibrated Wratten neutral density filters. Rates were calculated with 100, 72, 54, 39, 15 percent of maximum irradiance.

4. Determine Amount Glass Plate is Lifted During Continuous Exposure: A 5 x 7 cm piece of film was placed emulsion side up on the image plane. A 7.5 cm x 5.4 cm x 0.3 cm glass plate was placed on top of the film and gently rubbed to squeeze air out from between the two surfaces. The time base was set at 0.1 sec and the memory used. The 31 frequency measurements were converted to distances by:

$$d_n \text{ (um)} = (f_n - f_o)/3940$$

From this the maximum movement was determined. Six measurements were made using fresh film. Then to determine the effect of thermal expansion and system drifting six base line measurements were made using pre-exposed film samples. Mean and variances were calculated for each set of data. The difference in these means represents the actual maximum separation caused by gas diffusion. Ninety five percent confidence limits were calculated for this difference. If zero was included in these limits it can be concluded that no movement due to gas diffusion was measured.

5. Determine If Exposure From Front or Back is Different: The glass plate lifting experiment as described in part D was performed with emulsion side of diazo film up and emulsion down. For each case distance moved vs. time was plotted. Each experiment was repeated three times. The plots are visually compared to determine if differences exist.

6. Correlate Plate-Film Separation With Irradiance: The plate separation experiments as described in part D were performed for several film plane irradiances. Irradiance was controlled with calibrated Wratten 96 neutral density filters. Separations with 100, 72, 39, 15 percent of maximum irradiance were measured.

V. RESULTS AND DISCUSSION: To establish credibility, the accuracy of the test apparatus will be discussed, then the experimental results reviewed and compared with theory.

A. Apparatus Evaluation: As discussed in section III the calculated accuracy of a plate-film separation or gas discharge measurement is $\pm$ 13%. This error is caused by inability to precisely calibrate the apparatus and not experimental variances. As the error is built into the apparatus it should remain relatively constant. Experimental variances could have been due to apparatus vibration, apparatus settling, oscillator drifting, thermal expansion during exposure and/or other causes. A summary of the variances are in table 2.

1. Apparatus vibrations were a problem during initial experiments, but were virtually eliminated using isolated techniques. Vibrations would be seen as fluctuations in the frequency measurements. Because the frequency counter integrates over a 0.1 second period and the sample rate is five per second only low frequency vibrations could be seen. Charts 2, 3, 6, and 7 contain all data points collected. The stability indicates that vibration is not a problem. Chart 2b contains an experiment requiring both a shutter opening and closing. No indications of these operations are apparent. The conclusion is that vibration was not a significant variant in these experiments.
2. After setting to nominal (9.9 - 10.0 MHz) the oscillator frequency was generally not stable; usually drifting toward lower frequencies. This implies an oscillator circuit drift or a closing of the capacitor plates. With the external capacitor disconnected the short term (6 sec.) oscillator drift was not measurable. Thus settling in of the capacitor assembly was the cause of instability. To reduce this effect the assembly, after adjustment, was left to settle until the frequency change over a six sec. period was less than 100 Hz. This equates to a 0.025 um change in capacitor separation. Residual drifting variances were accounted for by replicated base line measurements.

3. The major reason for oscillator frequency drift was thermal expansion caused by the radiant energy of exposure. The resulting drift toward lower frequencies was accounted for by the baseline measurements.
4. Thermal expansion does not explain the variances seen between experiments. Other unidentified causes contribute to this experimental error. These errors could be the result of adhesion between the film and the rubber diaphragm or glass plate. This could increase the force required for separation and/or decrease the area where gas is collected. As the adhesion condition would not be uniform experimental variations would result.

B. Experimental Results: The results will be given in the order described in Section IV and presented with 95% confidence limits. These figures do not include any correction for the $\pm$ 13% uncertainty. Charts are used to show typical results. One graph may be used to illustrate several experimental replicates. The plate will be that replicate which most closely matches the average. Also, when comparing one film to another the film sensitivities must be considered. Full (100%) irradiance is the same for all experiments however the rate this energy decomposes diazo molecules varies with film types. The half density times provide an indication of this sensitivity. Because half density time is inversly proportional to irradiance, it should be possible to normalize the data to a selected time. However, a linear relationship was not found to describe either gas diffusion rate versus irradiance or maximum plate-film separation versus irradiance. Normalization is only possible, for a very general analysis.

1. Gas Diffusion Rate During Constant Exposure: The results are summarized in table 3, and charts 2-4. The charts depict representative gas discharge (emulsion-up), base line (emulsion down), and difference data. The slope of the difference curves illustrates the gas diffusion rate at any time after

initiation of exposure. The gradual increase in diffusion rate after initiation indicates that gas generated is delayed within the emulsion before omission. Because the emulsion was exposed from the rear the initial gas generated had to migrate through the emulsion thus accounting for this delay. Gas generation rate within the emulsion should be the greatest at the beginning of exposure because of the larger probability a photon will be absorbed; more diazo molecules are present.

2. Gas Diffusion After Exposure: Three replicates of a gas diffusion experiment were made where the exposure was terminated after 3.0 seconds. A typical result is shown in chart 2b. As can be seen the gas diffusion rate does not go to zero after exposure, therefore, gas release is not instantanious with diazo molecule decomposition. This substantiates the delay seen in the full exposure experiment.
3. Diffusion Rate Versus Irradiance: Chart 5 illustrates gas generation vs. time for 2620P7 film at five levels of relative irradiance. These curves are the point-by-point differences of the gas discharge and baseline data closest to average. To make this data more meaningful the diffusion rate was plotted vs. relative irradiance (chart 6b) and also vs. time to half density (chart 6a). The charts depict the 95% confidence intervals for each data point.
4. Plate-Film Separation: The results are shown in table 4 and charts 7 and 8. For the K&E positive and Scott Graphics materials the movement by gas diffusion and thermal drift, and by thermal drift alone were relatively close. With a sample size of 6 pairs it could not be shown that the plate and film seperated when using the Scott Graphics P4-150 film. Considering the sample size and variance there was a 90% confidence that if a separation of 0.12 um had occurred it

would have been detected. For the K&E material certainty of separation caused by exposure exceeded 95%. However, this separation was small, at most a third wave length of exposing radiation.

5. Determine Difference Of Front And Rear Exposure: Representative results of gas separation plus thermal expansion are illustrated in charts 9 and 10. For both types of film evaluated a clear difference exists between exposing the film from the front or rear, i.e. emulsion down or emulsion up. This difference does not occur in the total separation but in the initial separation rate. When the emulsion is exposed from the rear the bottom diazo molecules are most probably destroyed first. These molecules must diffuse through the emulsion before they can cause plate separation. With the exposure from the front, top molecules are exposed first and less diffusion is necessary. This explains the difference in the rate initial separation occurs and also correlates with the gas diffusion experiments.

6. Plate-Film Separation Versus Irradiance: Results are shown in table 4, and charts 11, 12, and 13. Chart 11 contains representative plate separation data for each exposure condition. The point-by-point difference between gas plus thermal movement and thermal movement only is plotted. To make the data more meaningful it was re-plotted in three ways; maximum plate-film separation vs. relative irradiance and time to half density (chart 12), and maximum plate separation vs. gas diffusion rate (chart 13). In each case 95% confidence limits for each data point was plotted. From chart 13, a one point correlation exists for the measured gas diffusion rate of K&E film and the measured plate separation with the 2620P7 data.

C. Theory Discussion: As shown in Section IIB the separation by exposure of a diazo duplication film and an original negative or positive, can be described analytically. Using the mathematical model theoretical separation vs. time plots were made employing measured gas discharge rates. These theoretical plots did not correlate completely with measured plate-film separations. Attempts were made to explain the differences.

1. Analytica Equation:

(a) From Section IIB:

$$a_t = \sum_{n=1}^{K+1} \left[22.4 \times 10^3 R - \frac{2\Delta P}{3\mu W} a_{n-1}^3 \right] \Delta t \quad \text{Contact Printer}$$

$$a_t = \sum_{n=1}^{K+1} \left[22.4 \times 10^3 R - \frac{\pi \Delta P}{3\mu LW} a_{n-1}^3 \right] \Delta t \quad \text{Rectangle}$$

Where: t = K t; exposure time (sec)

R; gas diffusion rate (mole/cm^2/sec)

P; mechanical pressure holding two films together (dynes/cm^2)

W; width of films (cm)

L; length contact surface (cm)

a; separation (cm)

μ; viscosity; 178 x 10^{-6} dynes/cm/sec for $N_2$7.

These equations can be written in the form:

$$a_t = \sum_{n-1}^{K+1} \left[B - C (a_{n-1})^3 \right] \Delta t$$

(b) At the beginning of an exposure the plate-film separation approaches zero. Thus the R(22.4 x 10^3) term will predominante and the increase in thickness with time will be linear. This is assuming that R is independant of time. As thickness increases so does the predominance of the second term (C $(a_{n-1})^3$). When the two terms are equal the separation will be constant. For low gas diffusion

rates maximum may not occur during exposure. In fact, the C $(a_{n-1})^3$ term may never be an issue. In this case the separation will be directly related to temperature and pressure. It is not anticipated that P will exceed 10^4 dyne/cm^2 and the temperature 320K, therefore, volume will always be very close to the volume at STP or 22.4 liters/mole gas. For very low gas diffusion rates: $a_t \cong Bt = (22.4 \times 10^3)\ Rt$.

2. Analysis Of Experimental Data:

(a) Separation vs. time plots were made using the rectangular gas flow equation for each gas diffusion rate corresponding to irradiances used in the plate separation experiments. A date time of 0.2 sec. was used. The size of the film samples 5 x 7 cm determined the width and length. Pressure was calculated by averaging the weight of the glass plate (31.7g) and the lower capacitor assembly (6.02g) over the area of the film sample. Delta pressure was 1.06×10^3 dynes/cm^2. The results of these calculations are shown in chart 14.

(b) Comparing this analytical with the experimental data differences and simularities are noted. The first difference is that the analytical results do not include the induction period. For the calculations, gas diffusion rate was assumed constant throughout the exposure. For correlating experimental with analytical results an approximation can be made assuming exposure commences after the induction period. This is not a bad assumption because during an operational exposure, energy strikes the film from the front and therefore no induction period is expected. Two additional facts come from the visual comparisons.

(1) The shape of the curves are similar.

(2) The maximums are within an order of magnitude, however, the differences can not be explained by experimental variances.

(c) Several attempts were made to explain these magnitude differences:

(1) It was first thought that they could have resulted from initial separations caused by a matte surface on the emulsions. Scanning electron microscope (SEM) photographs were made of the surfaces of the three positive working films. No matte was detected on the GAF or Scott Graphics materials. The K&E material had a slight matte. This surface had particles ranging from 0.25 to 1.5 um in diameter with about 30 particles in a 100 sq. um area. As no matte surface was detected it could not explain the separation differences seen in the GAF material. The matte seen on the K&E material could partially explain the differences there. The contradiction is that a separation was not detected for the Scott Graphic material even though it had no matte and the gas diffusion rate was very close to that of the K&E product.

(2) The next question was to consider if the plate lifted parallel from the film during exposure. for the GAF 2620P7 film an average measured maximum separation was 2.1 um. The calculated separation was approximately 8 um. If the plate lifted at an angle with one edge touching, the maxium separation at the other edge would only be 4.2 um with the center raised 2.1 um. Thus a non-parallel lift cannot explain difference.

(3) Incorrect constants or pressure values could not explain the difference for two reasons. For 2620P7 the differences were not linear; that is inserting corrected constant for one value does not correct the other three differences. For the K&E film the separation is always small and therefore the B term in the equation predominates. Thus any change in a C term constant would have negligable effect. The C term contains these constants.

(4) There is a high degree of certainty that the experimental measurements are correct and the theoretical calculations approximates plane, parallel film separations. It is also certain because of separation cubed dependency that experimental distance measuring error cannot account for these analytical experimental differences. The only conclusion is that the analytical equation does not describe the experiment. It is suspected that the film was not flat, that it was warped. This would produce varying separations across the format. No attempt was made to prove this hypothisis.

VI. CONCLUSIONS: The purpose of these investigations was to investigate nitrogen generation by diazo films during exposure and to correlate this gas generation with possible film-film separations in diazo contact printers. Several facts were generated during the experiments. These facts will be used to predict what may happen in a high speed contact printer.

A. Several Conclusions Were Reached From The Experiments:

1. Gas, presumably nitrogen, is released from the surface of diazo films during exposure. The rate of release depends upon intensity of exposure, type of diazo film, and whether the exposure is through the emulsion or base side of film.
2. Gas release is not instantaneous. The gas, after generation by diazo decomposition, must diffuse through the emulsion before release.
3. Gas diffusion can cause a glass plate to separate from the diazo film during exposure.
4. Analytical models were developed relating gas diffusion rates with film-film and plate-film separations. They are believed correct even though they did not correlate with measured plate-film separations. It is believed that the plate-film separation experiment was in error.

B. Using the experimentally derived gas diffusion rates and the analytical film-film separation equation estimates of separation in a high speed diazo printer were made. A high speed roll-to-roll diazo contact printer used to reproduce 12.7 cm wide originals may have an exposure time of one second. Also a contact pressure of about 10^4 dynes/sq cm could be expected. Using the gas diffusion rate data in table 3 and assuming a linear relationship between exposure and diffusion rate, rate estimates were made for GAF 2620P7, Scott Graphics, and K&E Positive materials for a one second to half density exposure. These were 2.2×10^{-8}, 3.07×10^{-9}, and 1.32×10^{-9} mole/sq cm/sec respectively. Using these estimates film-film separation versus exposure time plots were generated (chart 15). Expected separations at 1.0 seconds were 4.9 um for 2620P7, 0.69 um for P4-150, and 0.3 um for K&E positive.

C. These investigations showed that gas is generated during exposure for conventional positive working diazo materials. And, that this gas will cause film-film separations during contact printing. The experiments did not and were not designed to determine what a significant separation is with regard to image quality.

ACKNOWLEDGMENTS

I would like to thank Dr. G. Schumann, my research advisor and the Rochester Institute of Technology, Photographic Science Department staff for their assistance in completion of this project. I am also grateful to C. B. Krumm, Wright-Patterson AFB, for technical and material assistance. J. Meyers, Kodak Apparatus Division (KAD), Eastman Kodak Company provided vital assistance with fluid dynamics theory. Numerous other KAD personnel provided technical and morale support.

REFERENCES

1. M. L. Maskowitz and C. S. Saunders, Jr., private communication.

2. C. B. Krumm, private communication.

3. M. Dinaburg, "Photosensitive Diazo Compounds", Focal Press, N. Y., 1964, pp. 52-54.

4. D. P. Habib, "Dry Negative-Working Imaging System Based on Diazosulfonates", Symposium III Unconventional Photographic Systems, Preprint, 1971, pp. 98-98.

5. "An Evaluation of Scott Graphics Type P4-150 Film (POS)", Wright-Patterson AFB, OH, April, 1975.

APPENDIX

ELECTRONIC ASSEMBLIES

GENERAL:

The electronic assemblies provided the timing, frequency determination and memory functions necessary to support the experimental apparatus. The assembly was designed as a system of moduals. Each modual is a separate printed circuit (PC) card. And is attached to the main assembly via edge connectors and conventional wiring (Figure A-1).

Each modual provides a specific set of functions. This simplified construction as a specific function (i.e. timer counting) could be used more than once. Also moduals were designed with as much flexibility as thought practical. This was to ease accommodation of design changes as the experiments progressed.

Moduals were constructed on PC boards that were manufactured using photographic techniques. The circuit layout was made using press-on patterns and plastic film. From this a master Kodalith contact print internegative was produced. For transfering this pattern to a copper clad PC board GC Electronics etch resist sensitizer was used. This sensitizer is sprayed on the copper clad board. After drying it is contact printed using the Kodalith circuit pattern and the metal halide lamp used in the experiment. This resist is presumed to be a photo-polymerization type; the unexposed areas are removed with a solvent containing xyline. After the resist pattern is dryed unwanted copper is etched using a 30% ferric chloride solution. After drilling the etched PC board, the components were soldered on. Sockets were used for the integrated circuits (IC).

The following paragraphs will briefly discuss the functions of each modual. Schematics are provided in the attached figures. For persons who wish to understand the detailed operation, studying these circuit drawings is recommended. To aid this study manufacturers data books describing the ICs' operations is essential. Comment: TTL ICs were used except for the memory function.

OSCILLATOR (Figure A-2): This is a Colpitts type oscillator designed to operate at about 10MHz. The tuning coil was made adjustable to allow adjusting the oscillator to 10MHz with a capacitance of about 25 uuf across it. The 7413 integrated circuit is a Schmidt trigger used to shape the oscillating signal so it can be accommodated by the frequency determination circuits.

POWER SUPPLY (Figure A-3): Three power supply moduals are used. Each delivers a regulated 5 $\pm$ .2 volts at up to one ampere plus a 15 volt unregulated source. The three moduals work from a single 12.6 volt transformer.

TIME BASE (Figure A-4): The time base is a crystal controlled 8MHz oscillator with a series of frequency dividers to provide outputs at 1MHz, 100KHz, 10KHz, 1KHz, 100Hz, 10Hz and 1Hz. The 10th harmonic of the 1MHz output is used for adjusting the frequency of the 8MH oscillator. It is compared with the 10MHz WWV broadcast signal using a compacitor mixer and shortwave receiver.

TIMER (Figure A-5): This unit is composed of a timer control modual, two timer counter moduals (can be expanded to 4) and a shutter release modual. It uses power supply and time base functions in conjunction with the frequency determination and memory assemblies. The timer provides a positive pulse of preselected duration for shutter timing. The positive side of the pulse initiates shutter open and the negative side shutter closed. This pulse can also be used to start or terminate frequency counting.

TIMER COUNTER MODUAL (Figure A-6): This modual is composed of a decade counter, BCD to 7 segment decoder and numeric display, latch for retaining a preselected value, comparator to match preselected with counted value, and a shift register for transfering data to memory modual. Depressing the set memory timer switch transfers the displayed numeric value to the latch. A "clear signal" sets the decade counter to zero. Timing counts increment the counter, "count out" is 1/10 the frequency of the input signal. Moduals' decade counters are connected in series. When the decade counter value matches the stored value in the latch a "match out" signal is

generated. The shift register allows transfering data to the memory. This function is controlled by the memory control modual. Note: Due to a design error this circuit does not permit displaying a timer value stored in the memory modual.

TIMER CONTROL MODUAL (Figure A-7): This modual clears the timer counter decade counters, starts the timing pulse, starts the timing count, and stops the timing pulse and timing count when a match signal is received simultaneously from each timer counter modual. Timing "count-in" is from the time base; a 10 Hz signal was used. Timing "count-out" goes to the first modual's decade counter. A 500 msec. time delay is built into the starting cycle to permit the clear function and to eliminate multiple starts due to switch contact bounce.

SHUTTER RELEASE (Figure A-8): These circuits receive the timing pulse and activate the shutter open and shutter closed magnetic latches. The positive side of the timing pulse activates the shutter open circuit and the negative side the shutter closed circuit. The magnetic latches operate on 115 volt AC current. They are switched using solid state relays that turn on only when the AC voltage signal passes through zero volts. This greatly reduces the emission of electromagnetic radiation caused by rapid energizing of the magnetic latch. Conventional magnetic relays were tried but they generated severe interference with other portions of the electronic assembly.

COUNTER/MEMORY ASSEMBLY (Figure A-9): The counter is a conventional type frequency counter. It is used to monitor the output of the oscillator. The memory records frequency readings at specific intervals so they can be redisplayed at a later time. Six decades (digits) and three sampling rates (1 sec, .1 sec, .01 sec) are available. Resolutions of 1 Hz, 10 Hz, and 100 Hz are possible with an upper frequency response (set by 7490 decade divider) of approximately 15 MHz. The counter can be used in a continuous or one shot mode. In the continuous mode frequency measurements are taken at two second intervals for the one second sampling rate and at 0.2 sec intervals for the 0.1 sec rate and 0.1 sec for the .01 sec rate. The memory records each frequency reading, up to 31 readings. After the memory

is full it ceases to record, thus preserving the first 31 data points. The recorded data can be redisplayed on the frequency counter numeric displays one data point of a time in the order acquired.

COUNTER MODUAL (Figure A-10): These six moduals count the frequency pulses, store the final count and display the value after the count is complete. The modual also contains a shift register to transfer data to the memory modual. Input pulses are counted with a decade counter and an output pulse one tenth the input pulse frequency is generated. Upon completion of a frequency counting sequence the count is stored in a parallel load shift register. This stored value is decoded and displayed. The decoder is provided with ripple blanking to enable suppression of leading zeros. The data stored in the shift register can then be serially transferred to the memory modual. All shift registers, timer counter and counter, are connected in series. The mode control determines if an input signal parallel loads the register or shifts it.

COUNTER CONTROL MODUAL (Figure A-11a and A-11b): This modual provides the many functions necessary for the various modes of frequency determination. Using time base inputs it generates the sampling time and for continuous operation the proper pause time between samples. For the .1 sec and 1 sec sample time the modual divides an input frequency of 10 Hz and 1 Hz respectively by two thus generating a square wave 0.1 sec high and 0.1 sec low or 1.0 sec high and 1.0 sec low. This sampling signal is provided to a gate to permit turning on and off test signal to the counters. For the .01 sec sample time a 100 Hz signal is fed to a decade counter. The output of this counter is a signal .01 sec high and .09 sec low. This sampling signal fed to the gate provides a .01 sec sample time every .1 sec. Prior to sampling a clear pulse is generated to set all counter modual decade counters to zero. After the sampling period is completed a set latch signal is generated which parallel loads the counter moduals shift registers thus displaying the count and initiates a memory cycle. Various stop and start controls are provided to permit both manual and automatic operation. Manual being push button and automatic being controlled by the timer. The circuit is designed so that the start and stop will only

occur when the sampling signal is low, thus the circuit will not stop or start in the middle of a counting cycle. With the one shot switch activated the frequency counter will upon a start command progress through one cycle then stop.

MEMORY MODUAL (Figure A-12): This modual receives and records (read) the serial data from the shift registers. In the right mode it transfers stored data to the counter shift registers to be displayed (write). The heart of this modual is a 1024 bit random access memory that is addressed by a 10 bit command. Each word of data contains two four bit time digits and six four bit counter digits for a total of 32 bits per data word. These are addressed to the memory using five of the 10 address bits. The other five bits are used for selecting the 32 data word locations. Two separate five bit biniary counters address the data bit and data word locations. (Bit counter, word counter.) A preset input sets the word counter to zero thus permitting the initiation of 32 memory cycles. A clock input increments the bit counters, thus changing memory address location. When the counter reaches 32 (binary 11111) a match out signal is generated and the word counter is incremented. When the word counter reaches binary 11111 it will no longer incriment, thus any following data entries will be repeatedly stored in the 32nd word memory location. The read-write inputs control the mode of operation.

MEMORY CONTROL MODUAL (Figure A-13): This modual controls memory cycle functions for recording or displaying one data word. It is initiated with a set latch signal from the counter controller or a manual cycle input. The manual cycle input, a push button, is used primarily for retrieving and displaying stored data. The modual generates, from a 100 KHz time base signal, a series of clocking, shifting, and read-write signals for memory modual operation. The sequence is different for read and write mode. Upon receipt of a set latch or manual cycle signal a mode signal is sent to each shift register to permit shifting. Then the sequenced timing pulses are started and continues to cycle until receipt of a match signal from the memory modual. This signifies that all bits have been stored and that the shift registers contain the same data as before the cycle started. Or, that all stored data for one data word has been entered into appropriate shift register. At termination of memory cycle the mode is switched low to permit parallel loading of shift registers.

FILM TYPE	TIME TO ½ DYE CONCENTRATION	PROCESS	DENSITOMETER
Scott Graphic P4-150*	6.8 sec.	Atlantic Processor	TD 504
P4-150	4.0 sec.	Atlantic Processor	TD 504
GAF 2620P7	2.6 sec.	Atlantic Processor	TD 102
GAF 2620P7	2.2 sec.	Ammonia Vapor Jar	TD 102
K&E	5.7 sec.	Ammonia Vapor Jar	TD 102
KODAK	3.7 sec.	Ammonia Vapor Jar	TD 504

* Using H 400 A33-1/T16 Mercury Vapor Lamp, All Others Used Metalarc 46, M 400BD Lamp.

TABLE 1a, Exposure Time To One Half Dye Concentration.

Filter Density	Effective Density (GAF 2620P7)
0.10	0.14
0.20	0.27
0.30	0.41

TABLE 1b, Effective Density Of Wratten 96 Neutral Density Filters.

	ACCURACY
Calculation of Delta Distances (Should be constant through experiments)	3940 Hz/um $\pm$ 13%
Drift During Exposure, No Film on Film Plane (Calculated from 4 samples)	(0.30 $\pm$ 0.05 um
Drift of Gas Discharge Apparatus (Effective gas rate)	
95% Probability -- 100% Irradiance	(0.014 $\pm$ 0.016) x 10^{-8} mole/cm^2 sec
72%	(0.019 $\pm$ 0.009) x 10^{-8}
54%	(0.012 $\pm$ 0.013) x 10^{-8}
39%	(0.010 $\pm$ 0.010) x 10^{-8}
15%	(0.005 $\pm$ 0.022) x 10^{-8}
Drift Due To Exposing Film Between Two Plates (Plate-Film Separation Experiments)	
95% Probability -- 100% Irradiance	(0.16 $\pm$ 0.09) um
72%	(0.17 $\pm$ 0.07) um
39%	(0.082 $\pm$ 0.082) um
15%	(0.043 $\pm$ 0.115) um
Effects of Shutter and Room Vibrations	None Detected.

TABLE 2; Calculated and Experimental Variances in Apparatus

FILM TYPE	IRRADIANCE (% of Max.)	GAS DIFFUSION RATE (mole/cm^2/secx10^{-8})	HALF DENSITY TIME (SEC)
GAF 2620P7	100	0.92 ± 0.04	2.4
	72	0.74 ± 0.04	3.33
	54	0.57 ± 0.03	4.44
	39	0.43 ± 0.02	6.15
	15	0.16 ± 0.01	16.0
Scott Graphics P4-150	100	0.033 ± 0.006	4.0
Scott Graphics P4-900 (Negative Working)	100	NONE DETECTED	NOT CALCULATED
K&E Positive Working (Unknown No.)	100	0.054 ± 0.006	5.7
KODAK Diazo M 4950	100	0.61 ± 0.03	3.7

TABLE 3, Summary of Gas Diffusion Rate Results.

FILM TYPE	IRRADIANCE (% of Max.)	PLATE-FILM SEPARATION (um)	½ DENSITY TIME (SEC)
GAF 2620P7	100	2.10 ± 0.41	2.4
	72	1.22 ± 0.49	3.33
	39	0.66 ± 0.28	6.15
	15	0.12 ± 0.11	16.0
K&E Positive Working (Unknown No.)	100	0.092 ± 0.088	5.7
Scott Graphics P4-150	100	NONE DETECTED	4.0

TABLE 4, Summary of Glass Plate-Film Separation Data.

Chart 1a

	L (10^{-6})	C (10^{-12})	δ (degree)
A	1.382	156.4	0.0
B	1.528	141.5	0.6
C	1.528	141.5	0.0
D	1.382	156.4	0.6

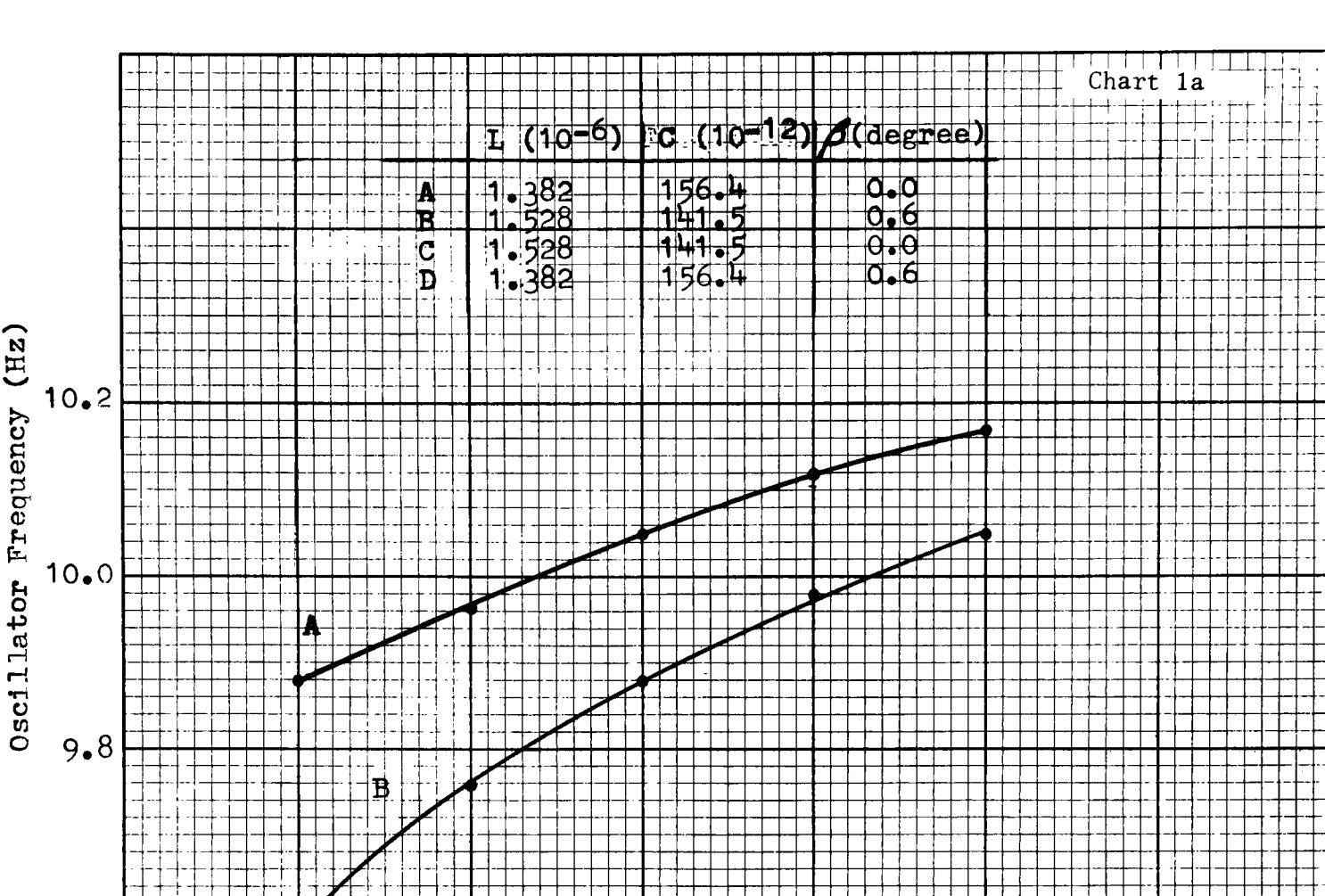

Chart 1b:
Capacitor-Oscillator
Calibration Plots

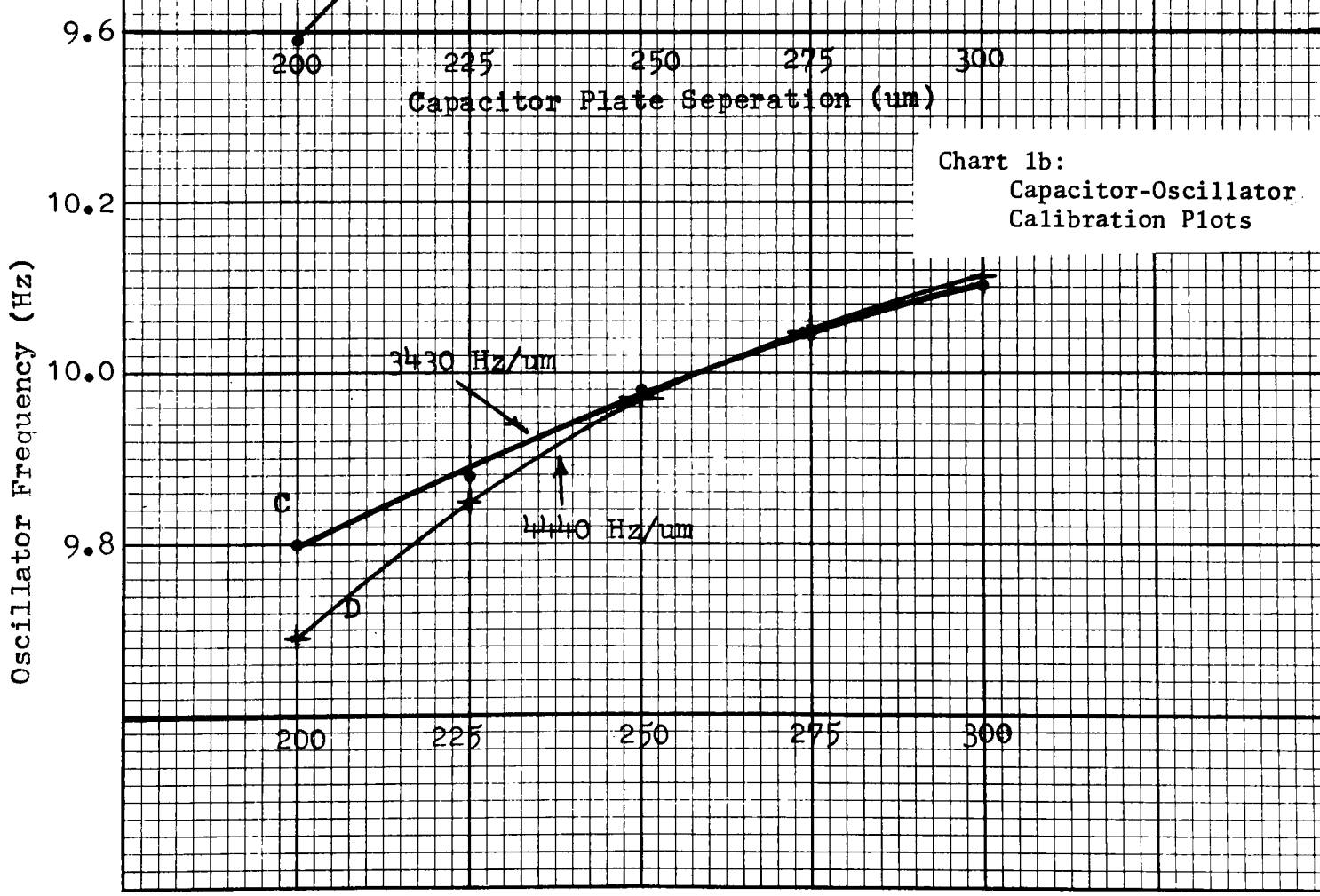

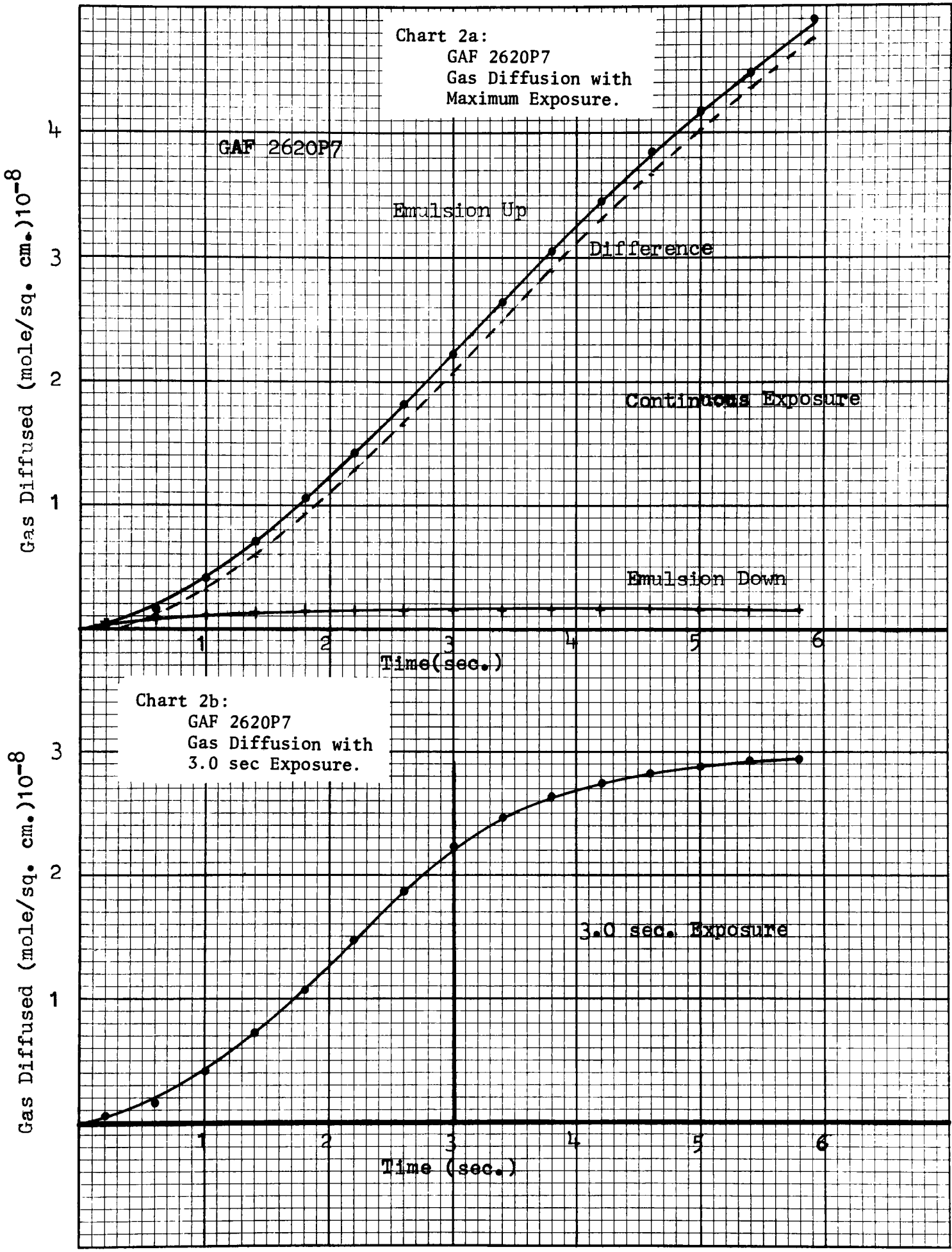

Chart 3a,b: Gas Diffusion with Maximum Exposure.

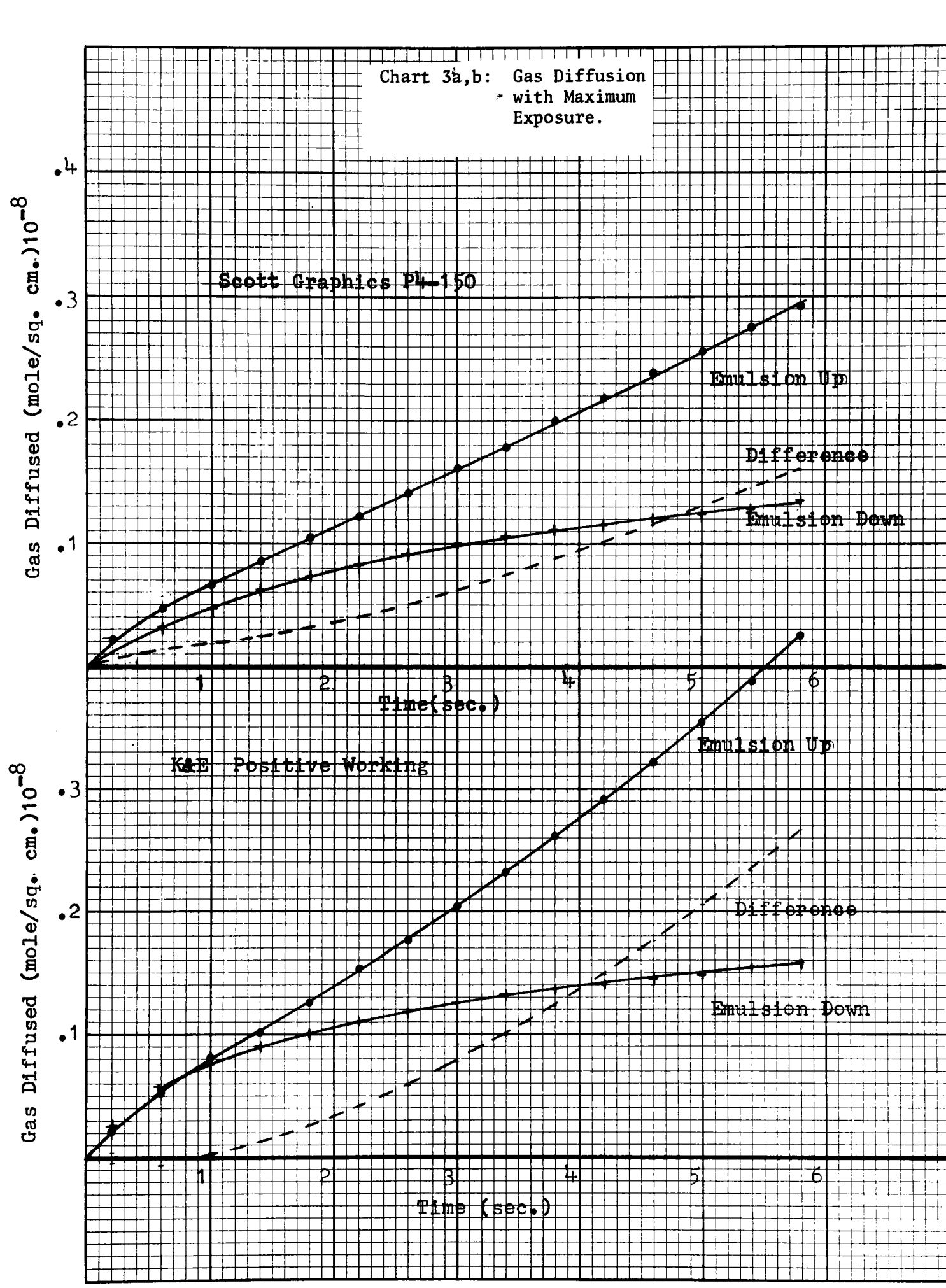

Chart 4: Gas Diffusion with Maximum Exposure.

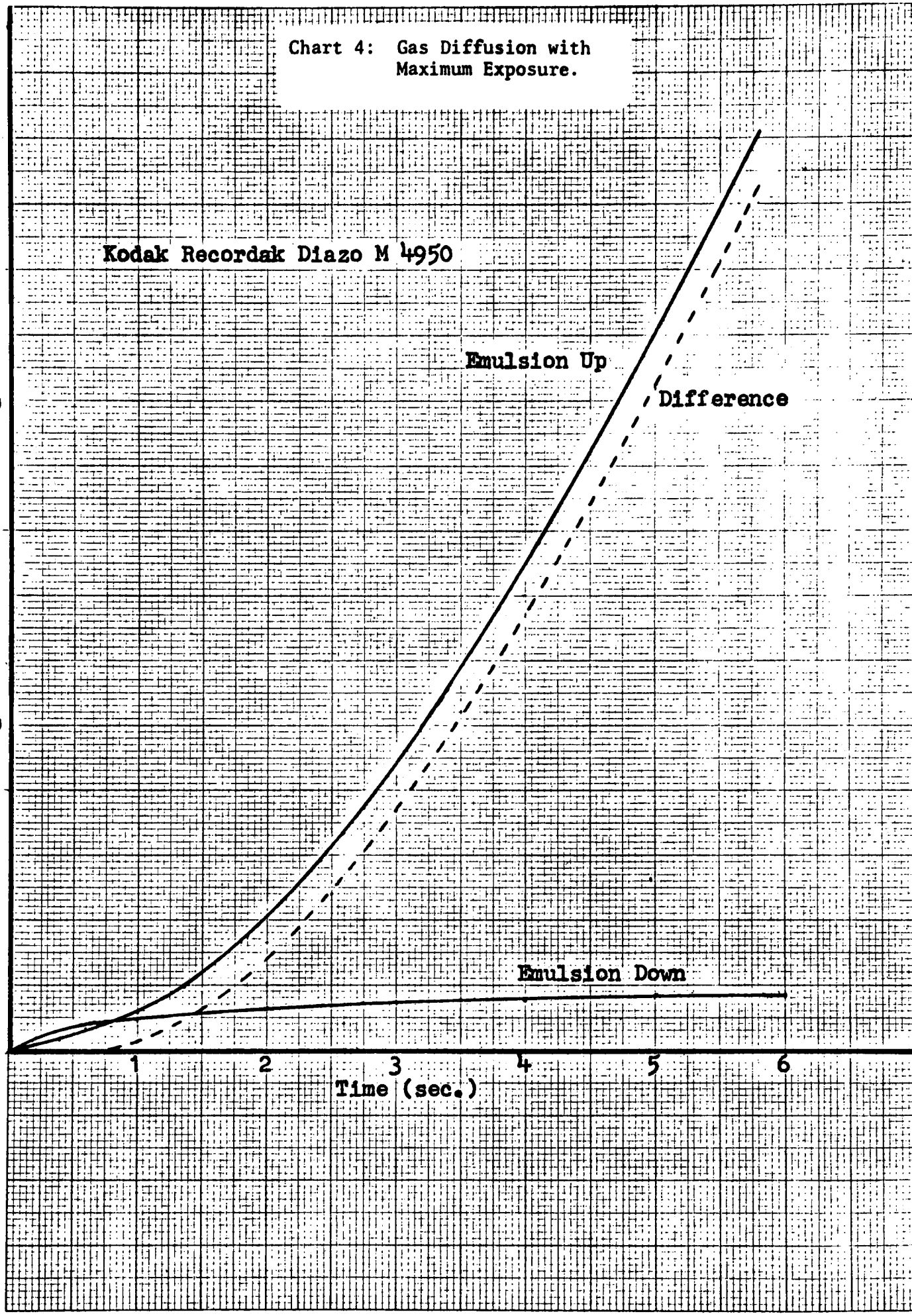

Chart 5: Gas Diffusion at Several Exposure Levels.

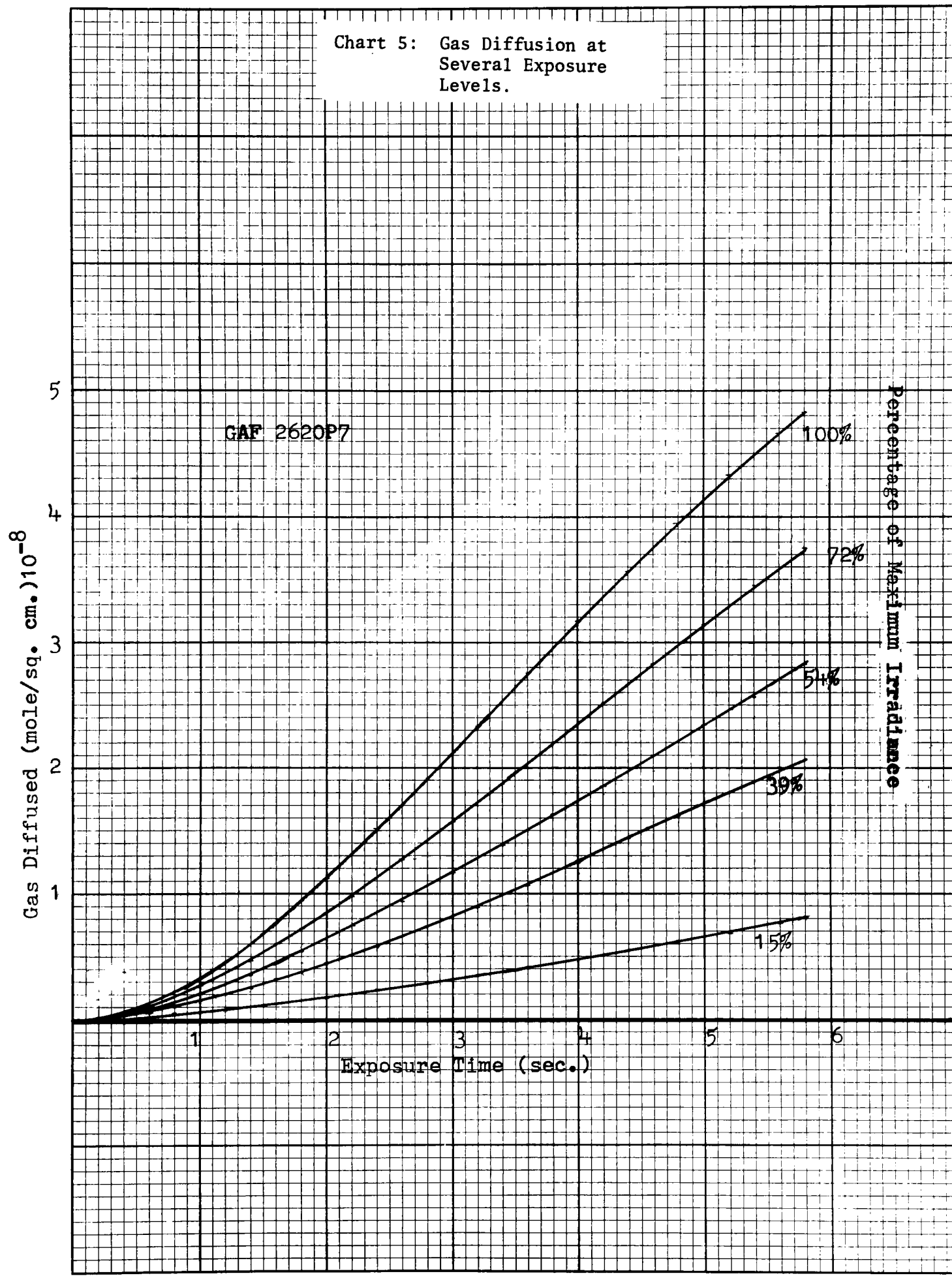

Chart 6a,b: Gas Diffusion Rate with Respect to Time to Half Density and Relative Irradiance.

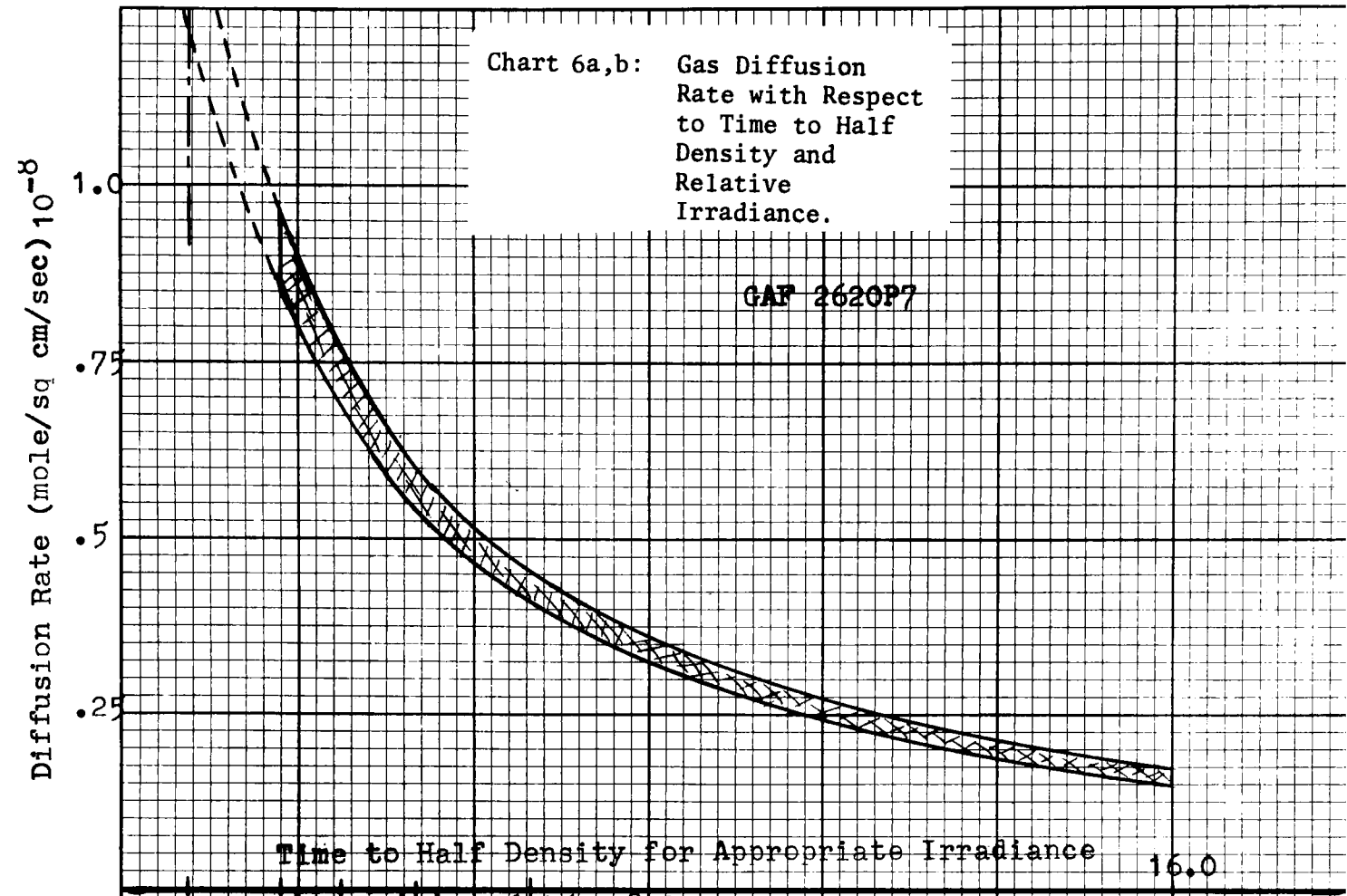

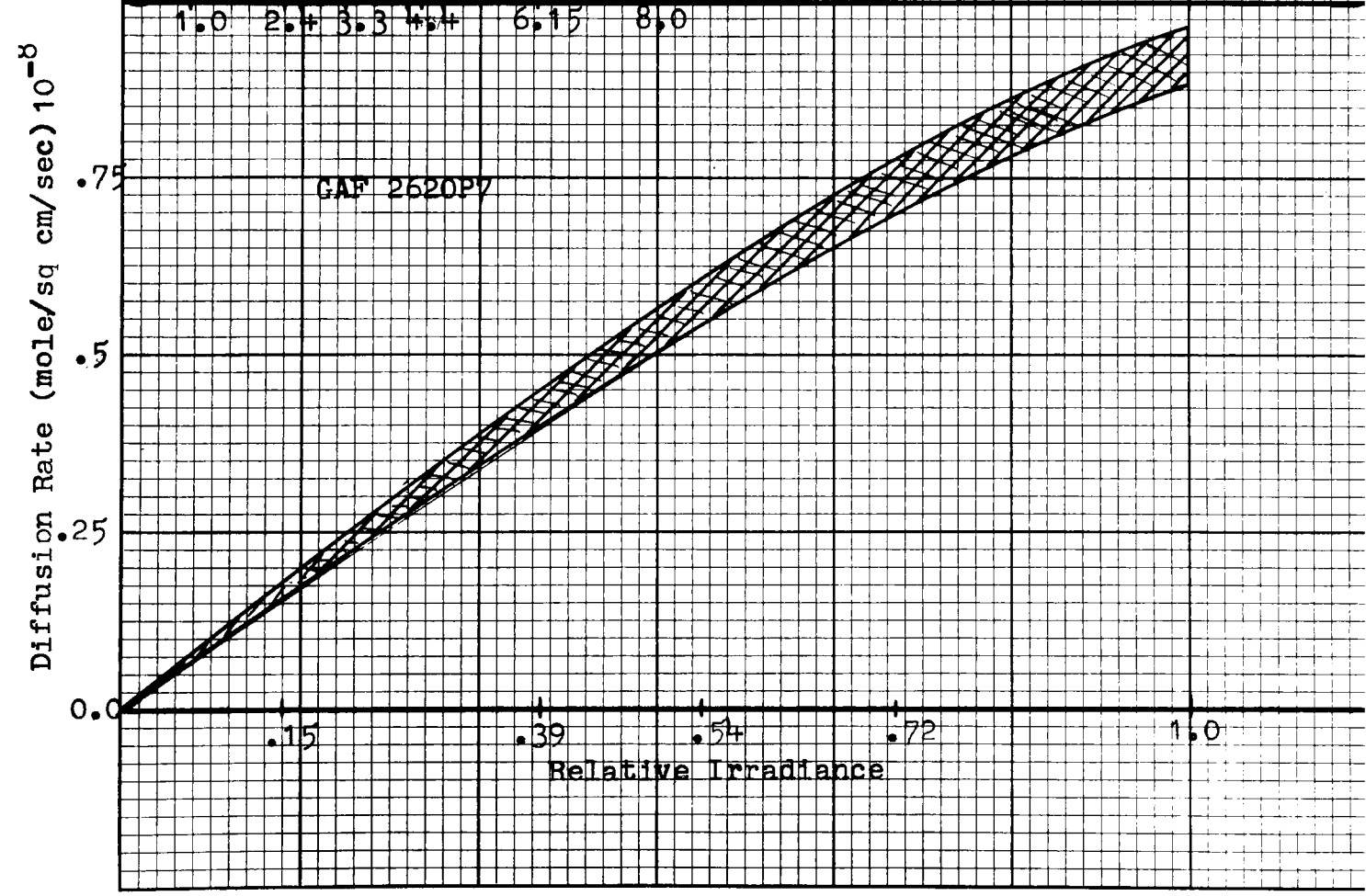

Chart 7: Plate-Film Separation at Maximum Irradiance with Fresh and Pre-Exposed Film.

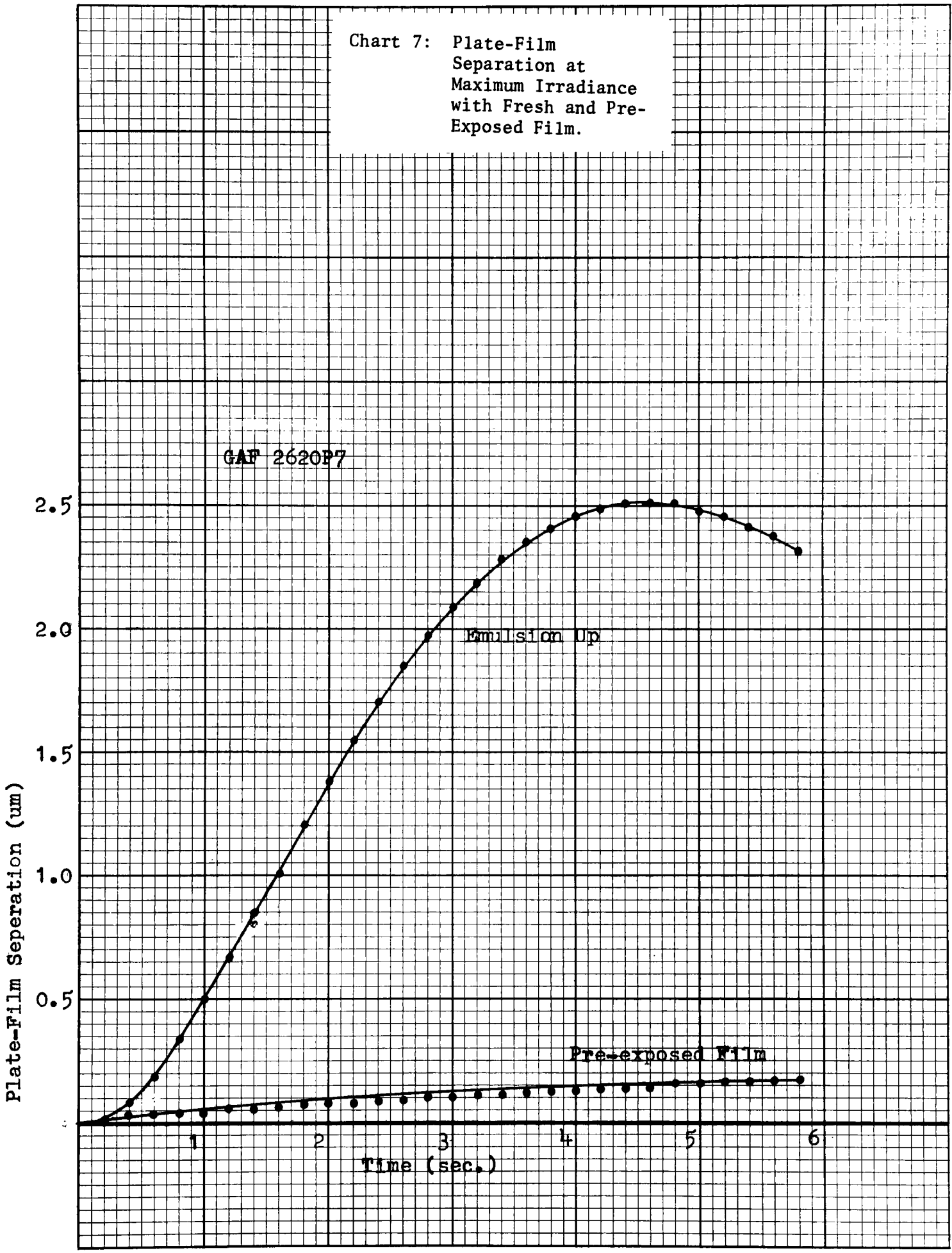

Chart 8: Plate-Film Separation at Maximum Irradiance with Fresh and Pre-Exposed Film

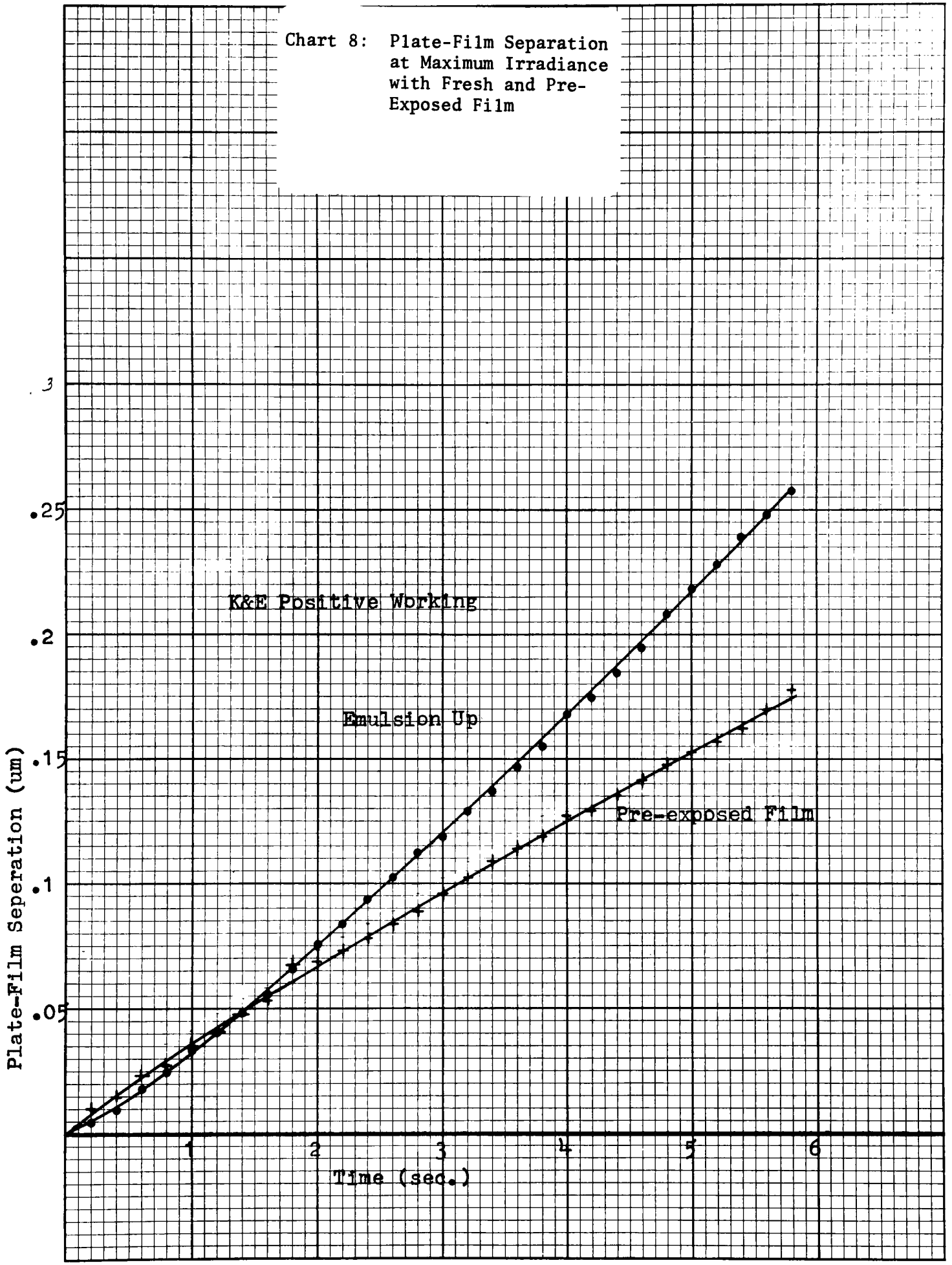

Chart 9: Plate-Film Separation for Maximum Irradiance at the Base Side and Emulsion Side of Material.

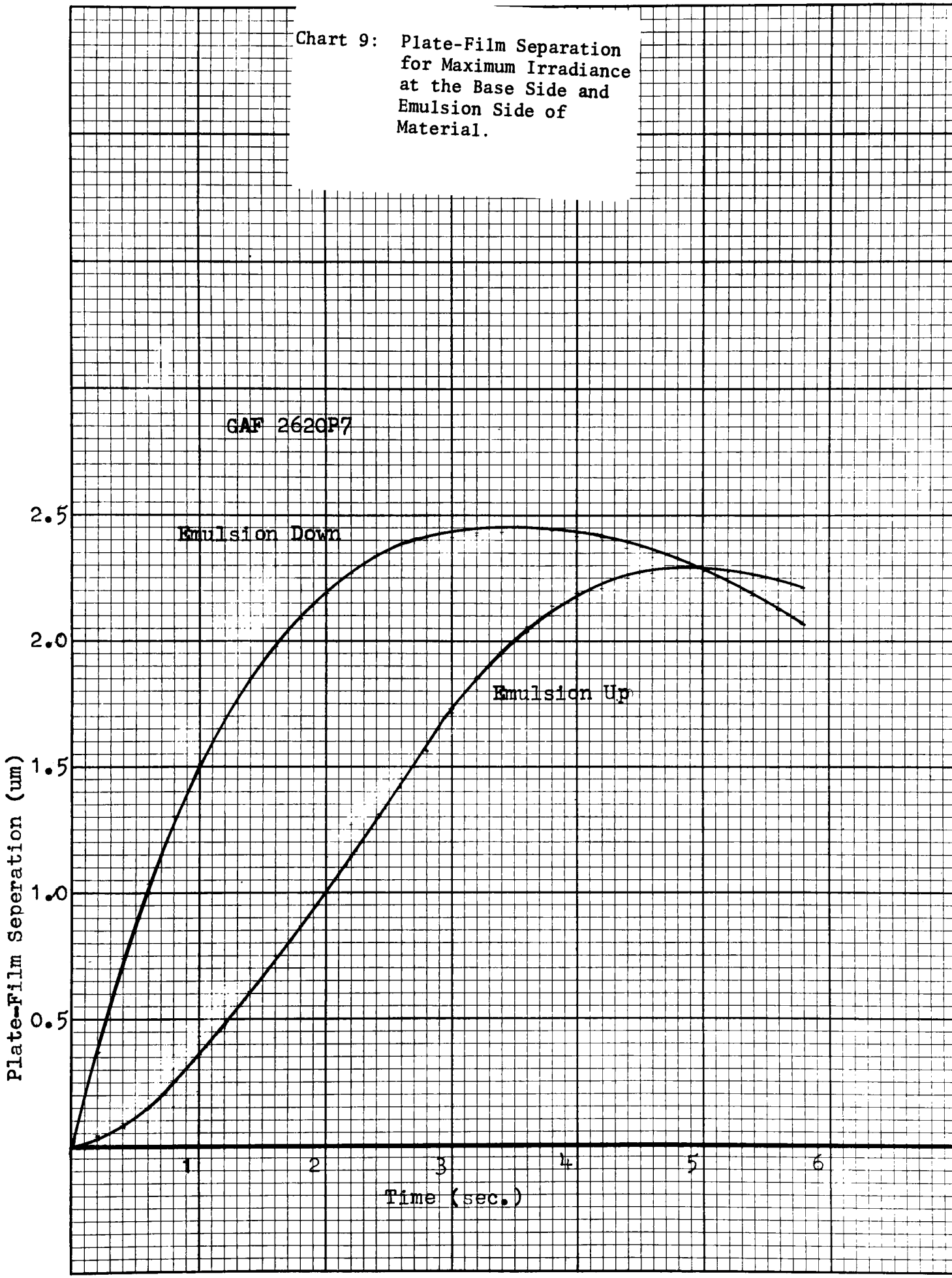

Chart 10: Plate-Film Separation Including Thermal Expansion for Maximum Irradiance at Base Side and Emulsion Side of Material.

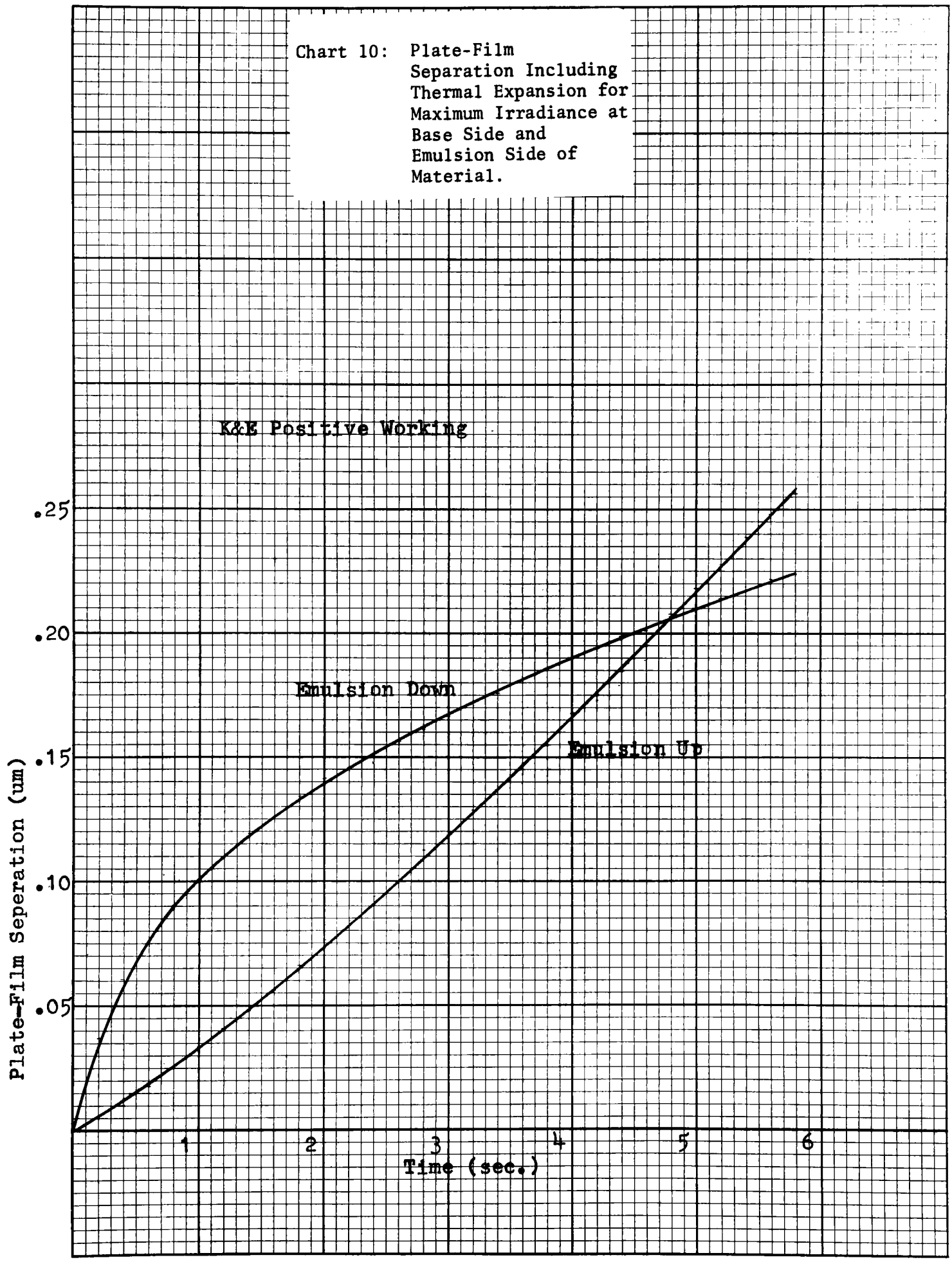

Chart 11: Plate-Film Separations at Various Relative Irradiances.

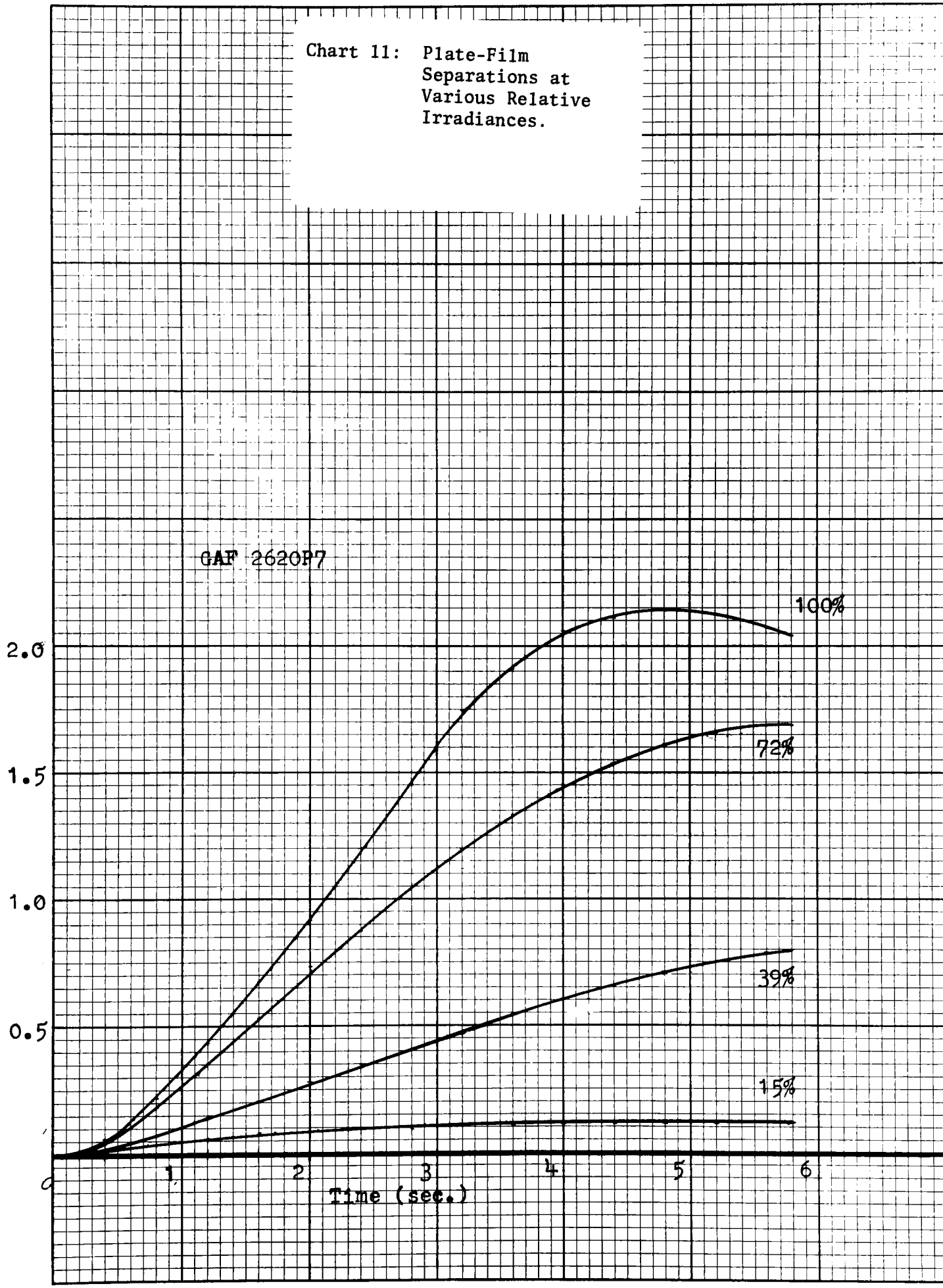

Chart 12a,b: Plate-Film Separation with Respect to Time to Half Density and Relative Irradiance.

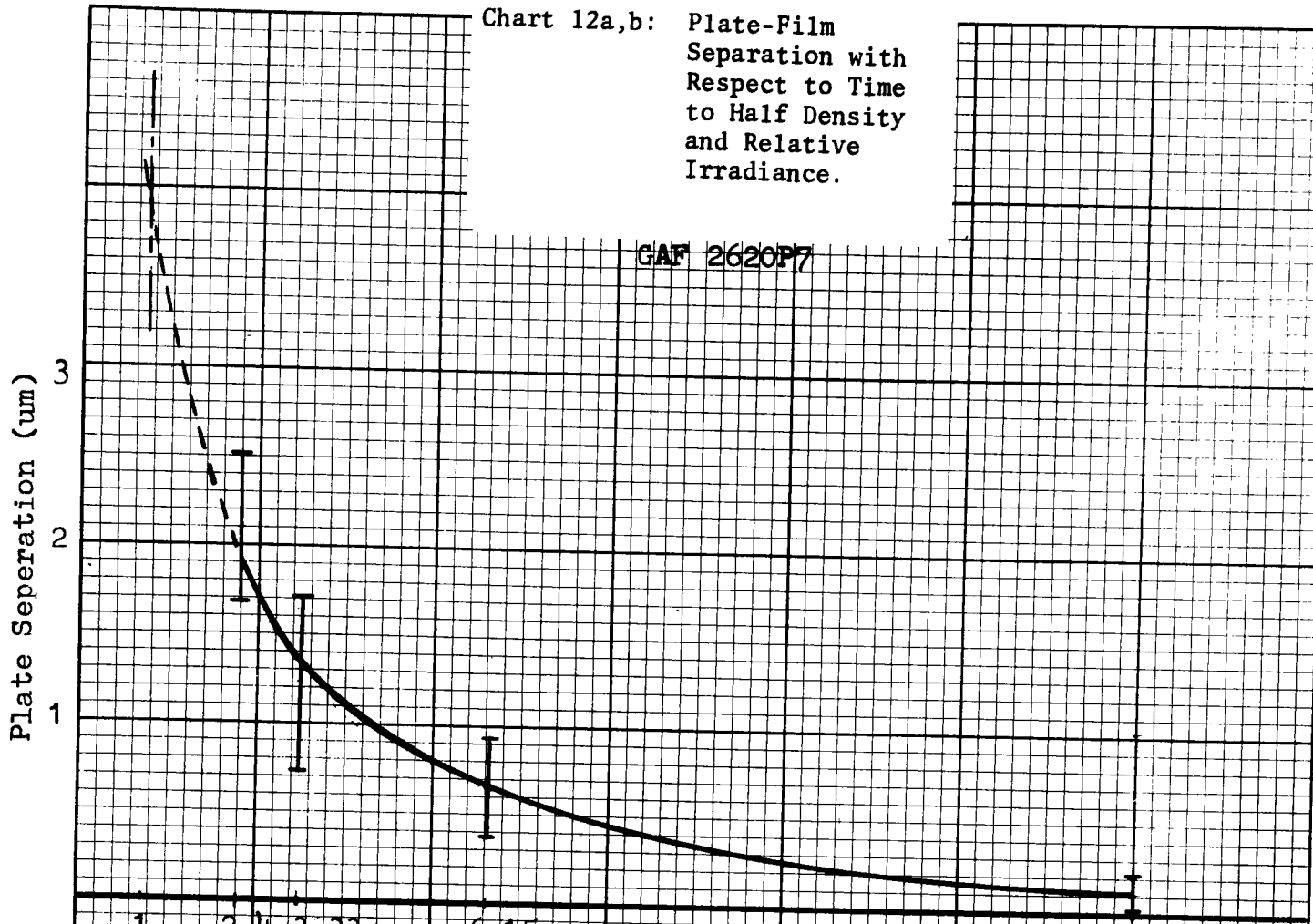

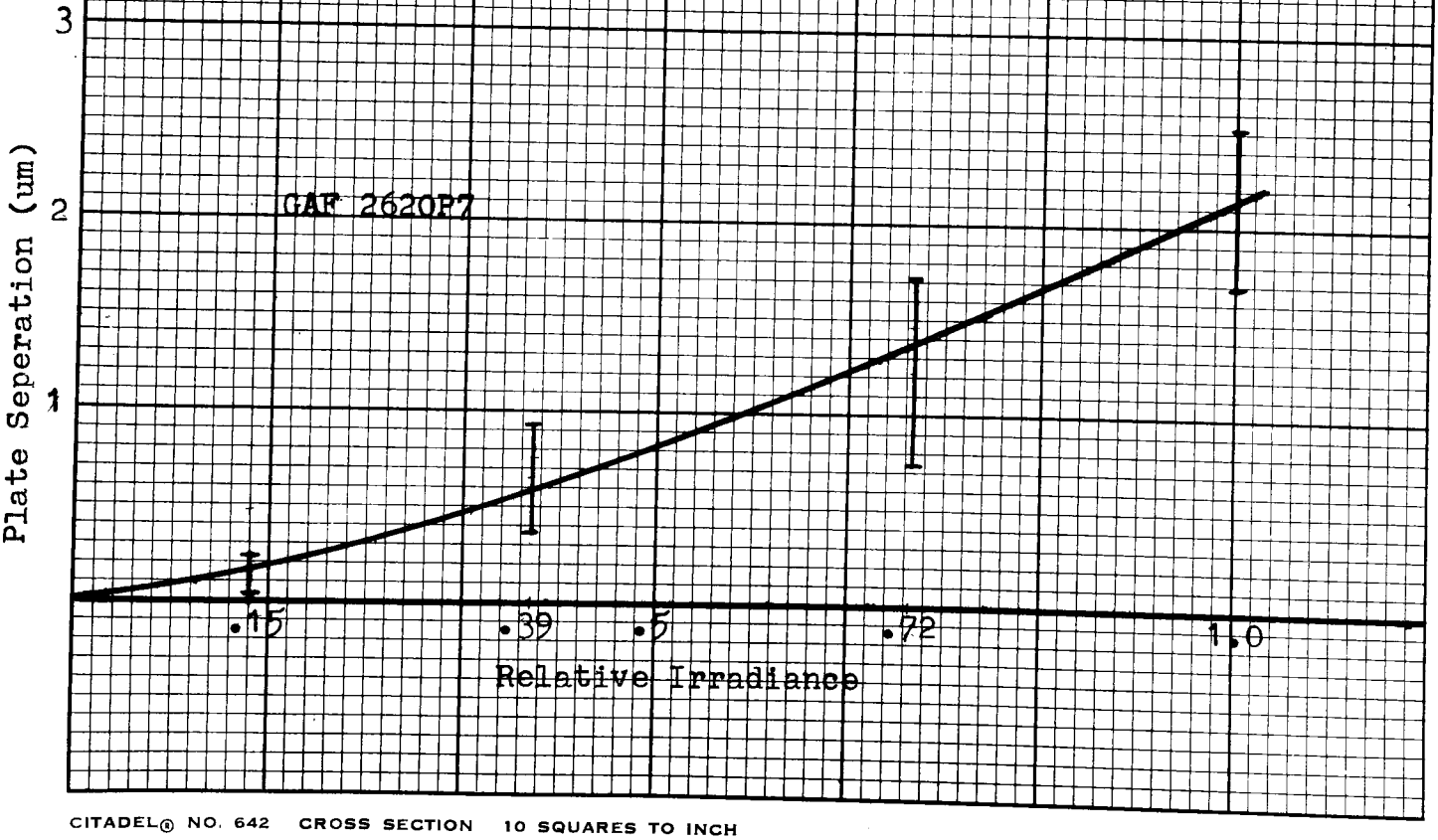

Chart 13: Plate-Film Separation with Respect to Gas Diffusion Rate.

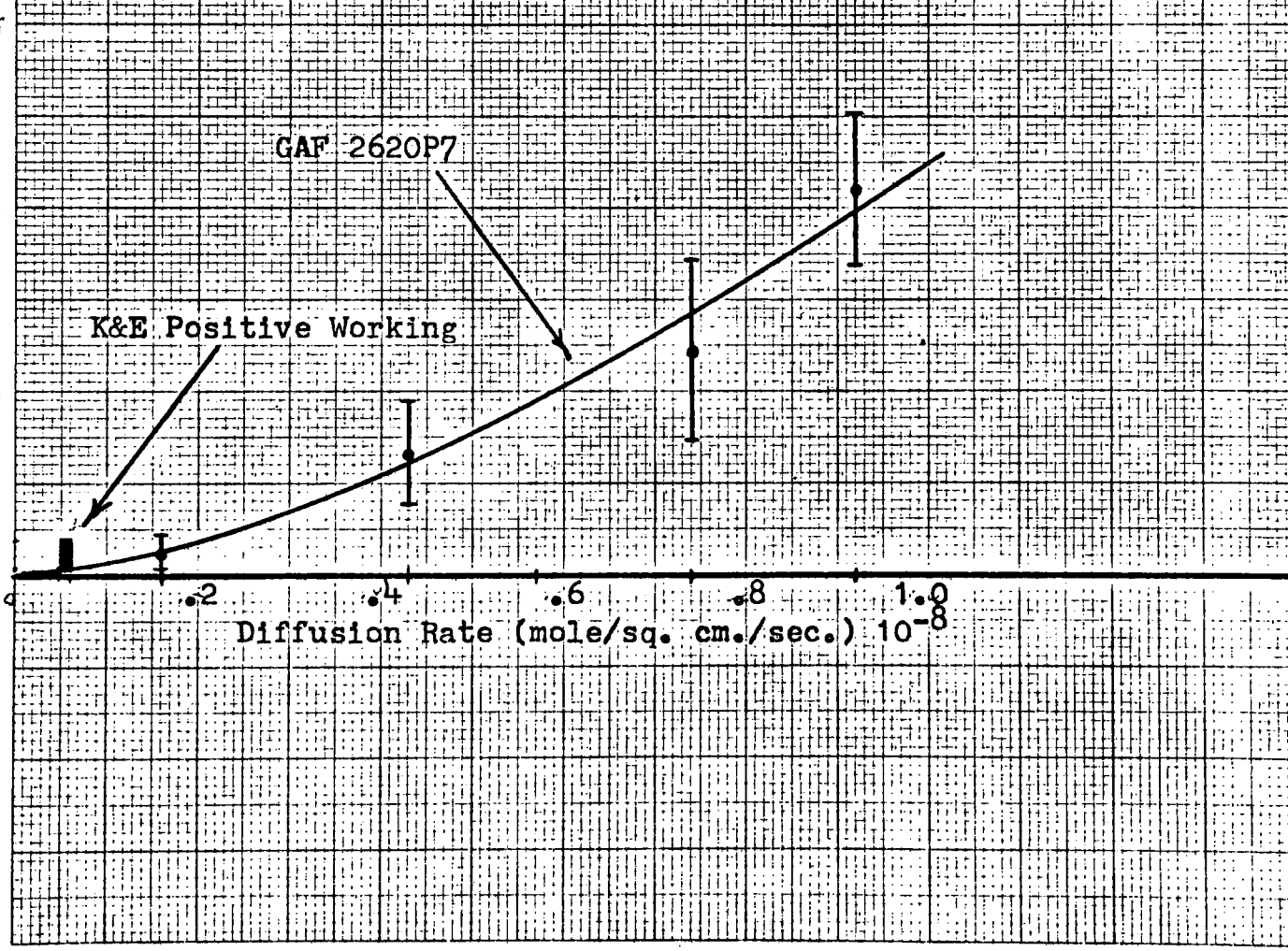

Chart 14a,b: Theoretical Plate-Film Separation Using Analytical Fluid Flow Equations and Experimental Gas Diffusion Data.

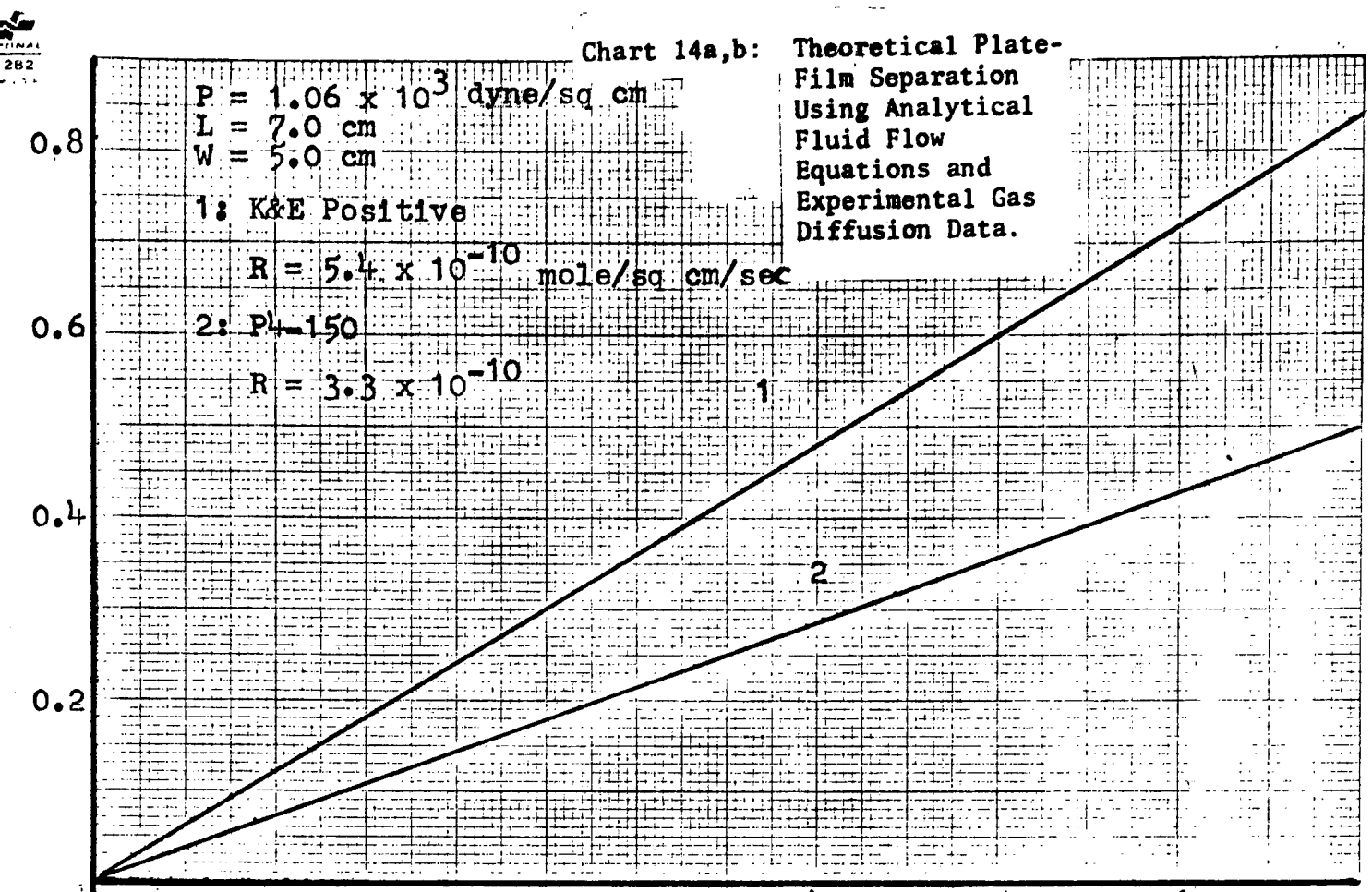

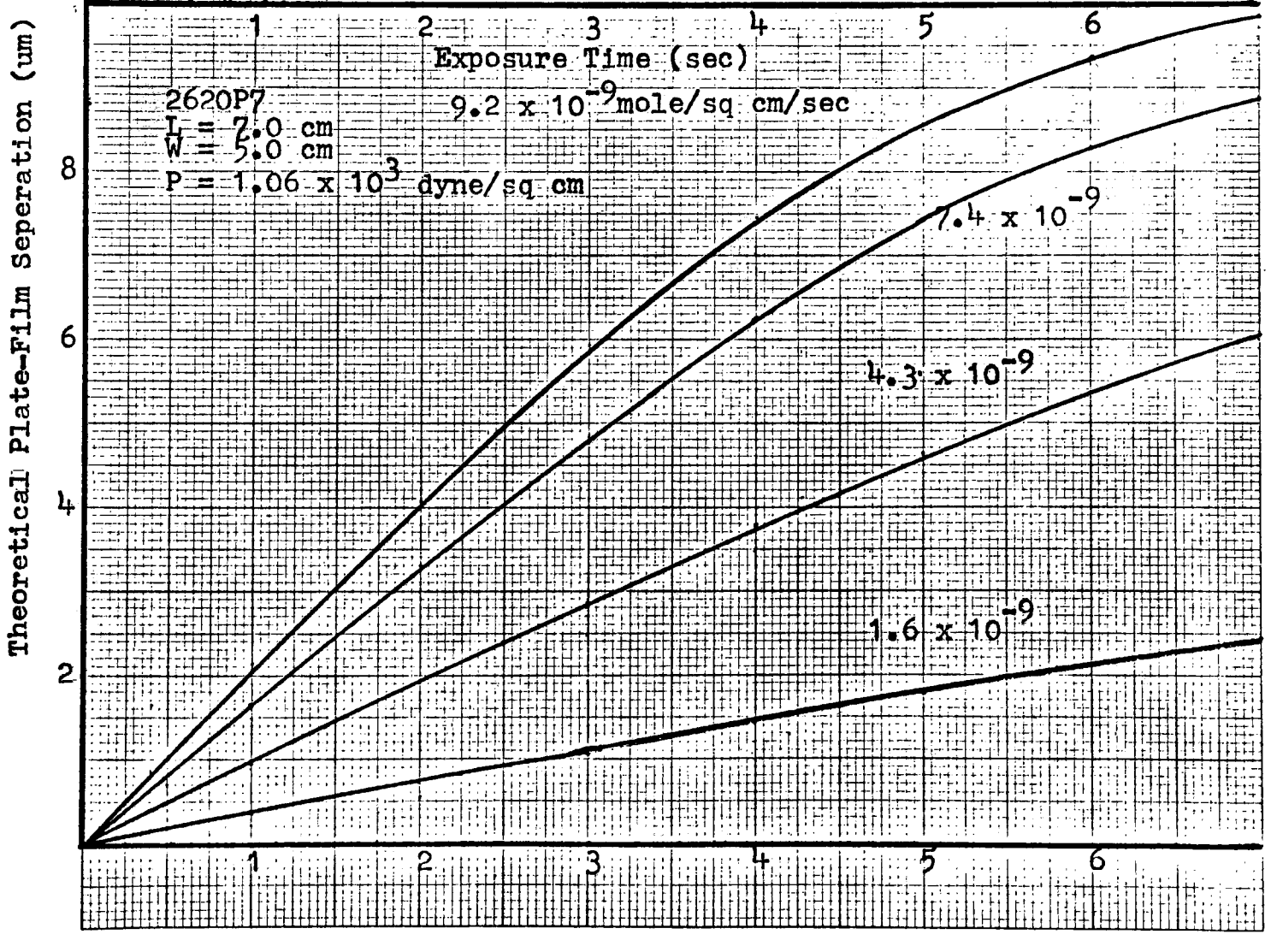

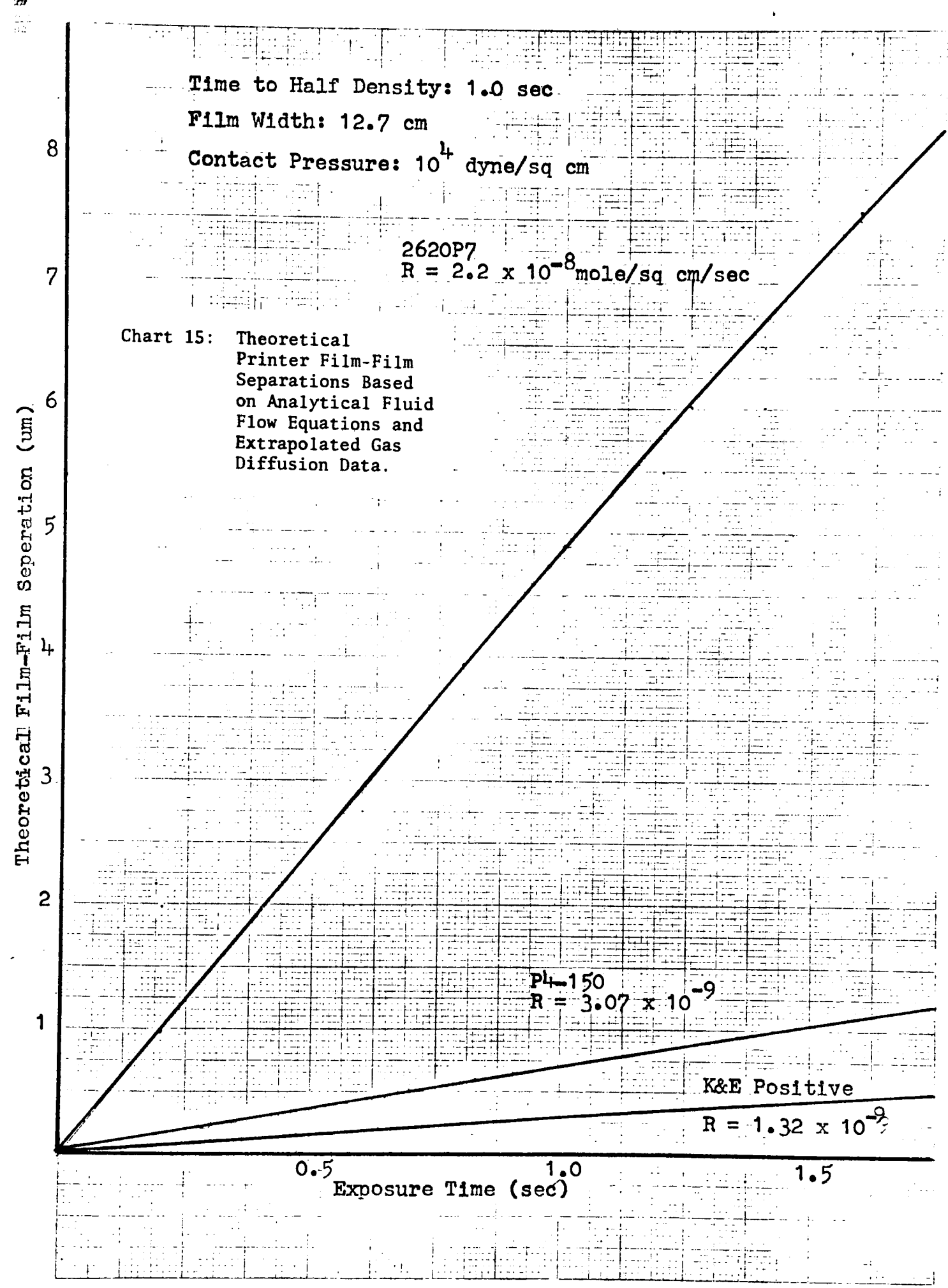

Chart 15: Theoretical Printer Film-Film Separations Based on Analytical Fluid Flow Equations and Extrapolated Gas Diffusion Data.

squares to the inch

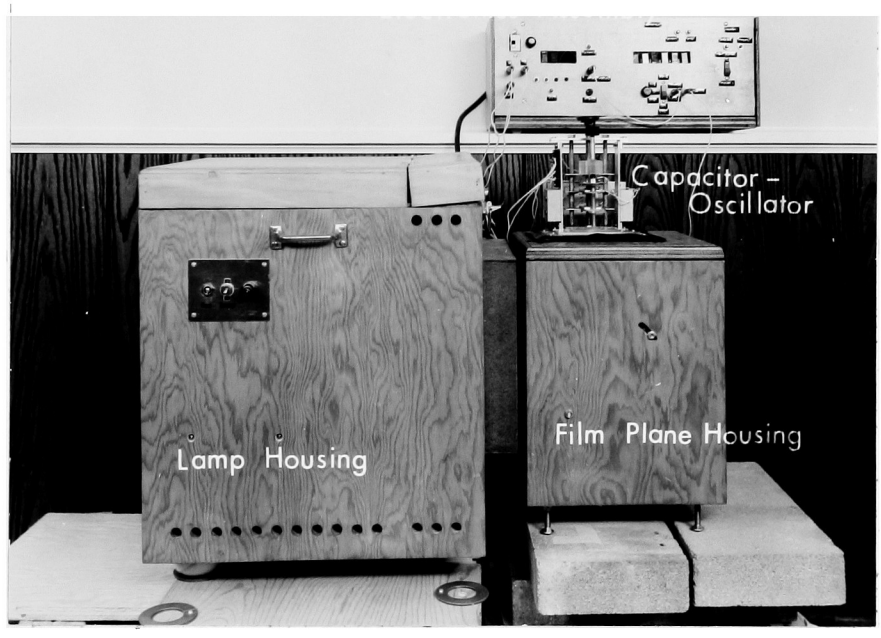

Figure 1: Test Apparatus

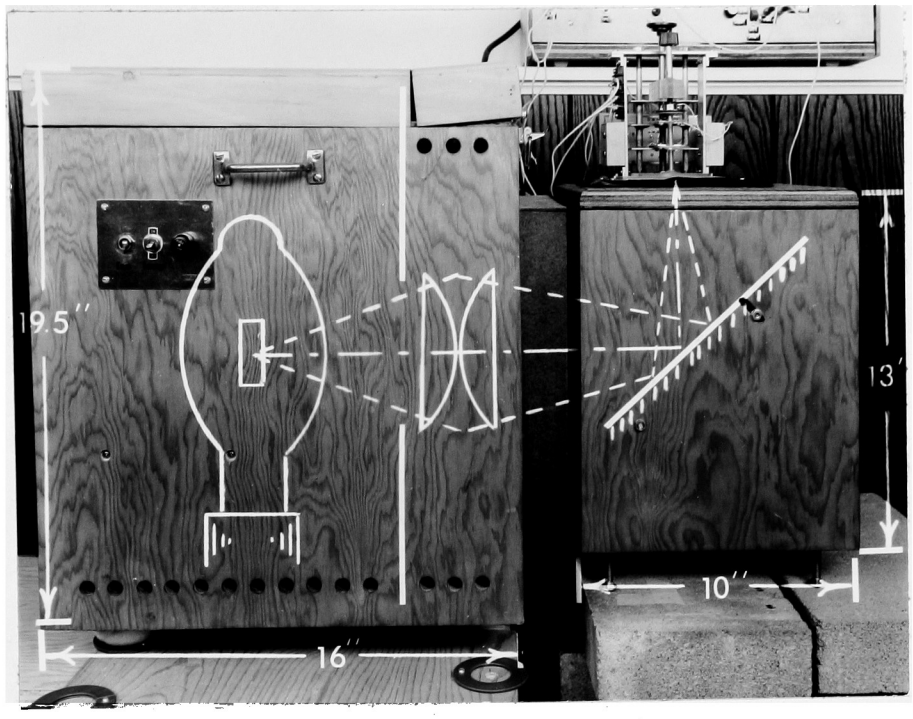

Figure 2: Illumination System

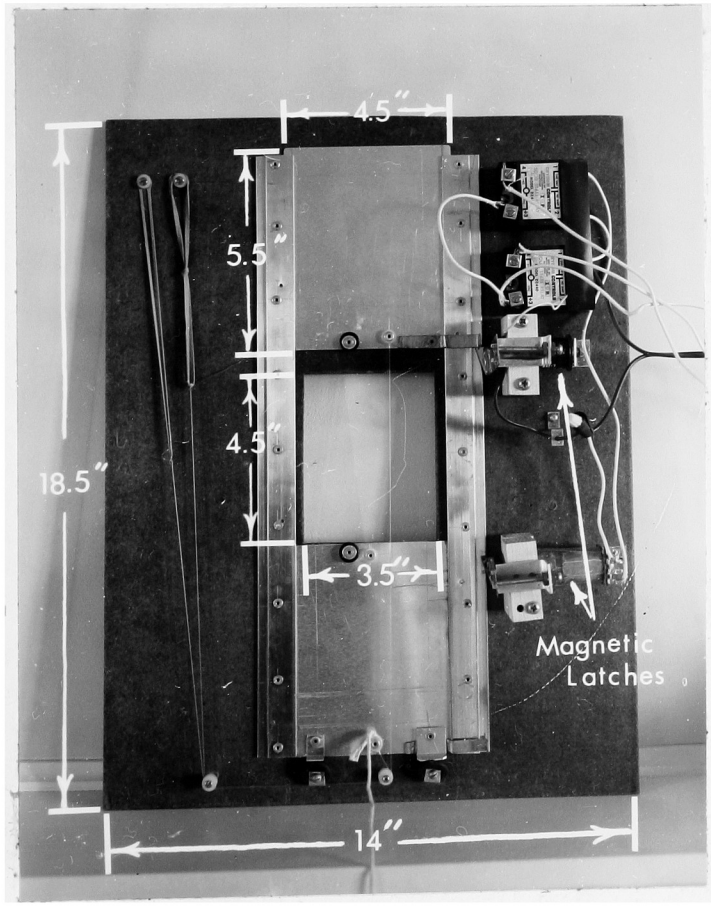

Figure 3:
Shutter Mechanism

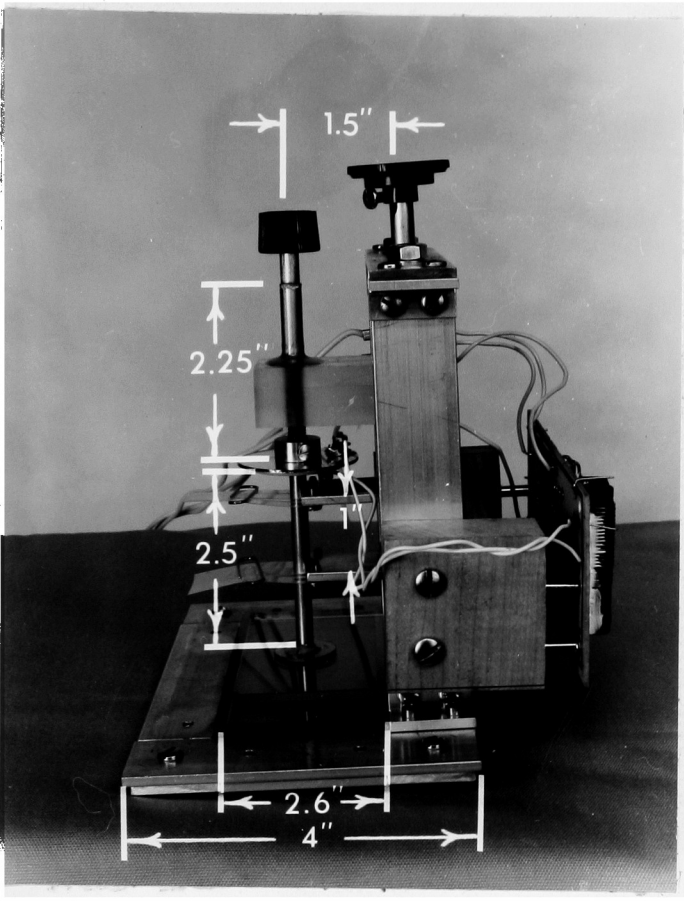

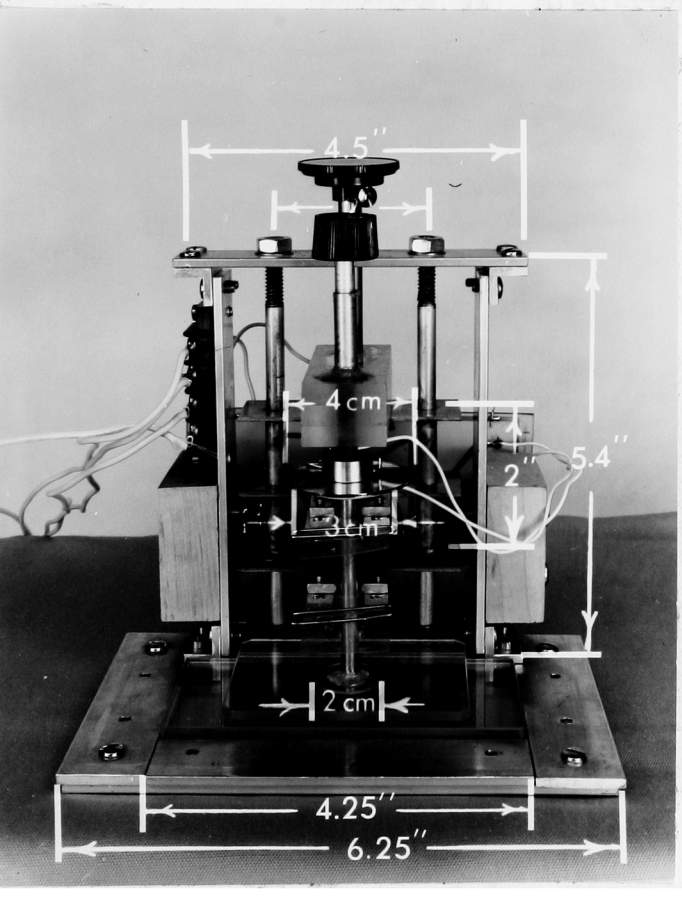

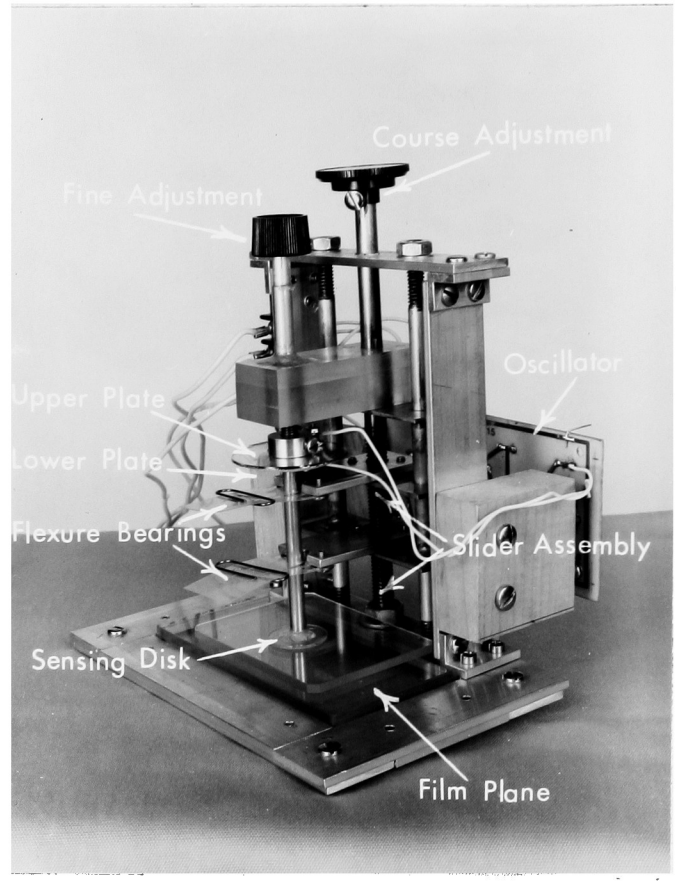

Figure 4: Capacitor-Oscillator Assembly

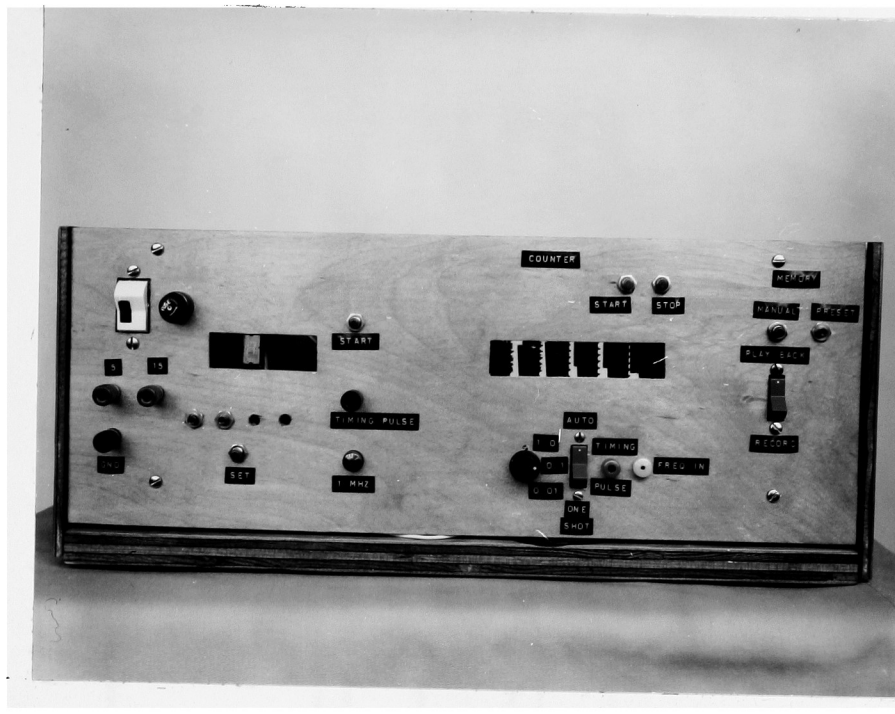

Figure 5: Electronics Assembly

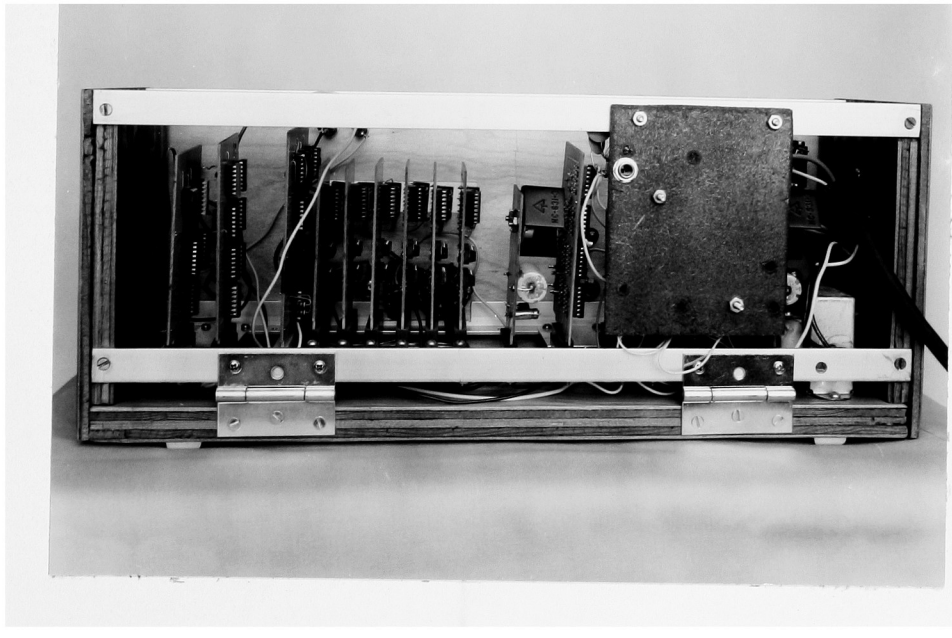

Figure A-1: Circuit Board Assemblies

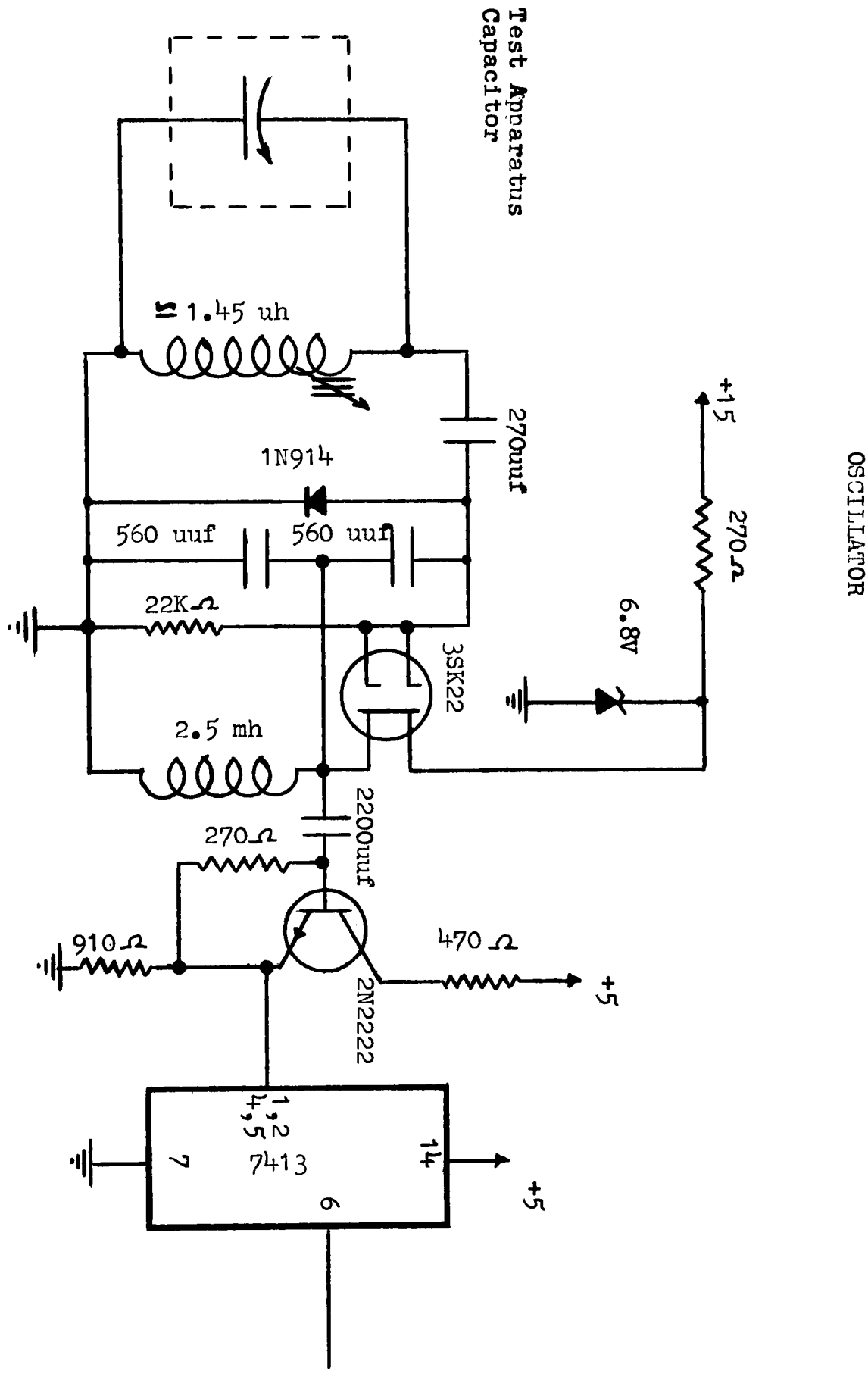
Test Apparatus Capacitor
1.45 uh
270uuf
1N914
560 uuf
560 uuf
22K
3SK22
+15
270
6.8V
2.5 mh
2200uuf
270
910
470
+5
2N2222
1,2
4,5
7413
7
14
6
+5
OSCILLATOR

Figure A-2

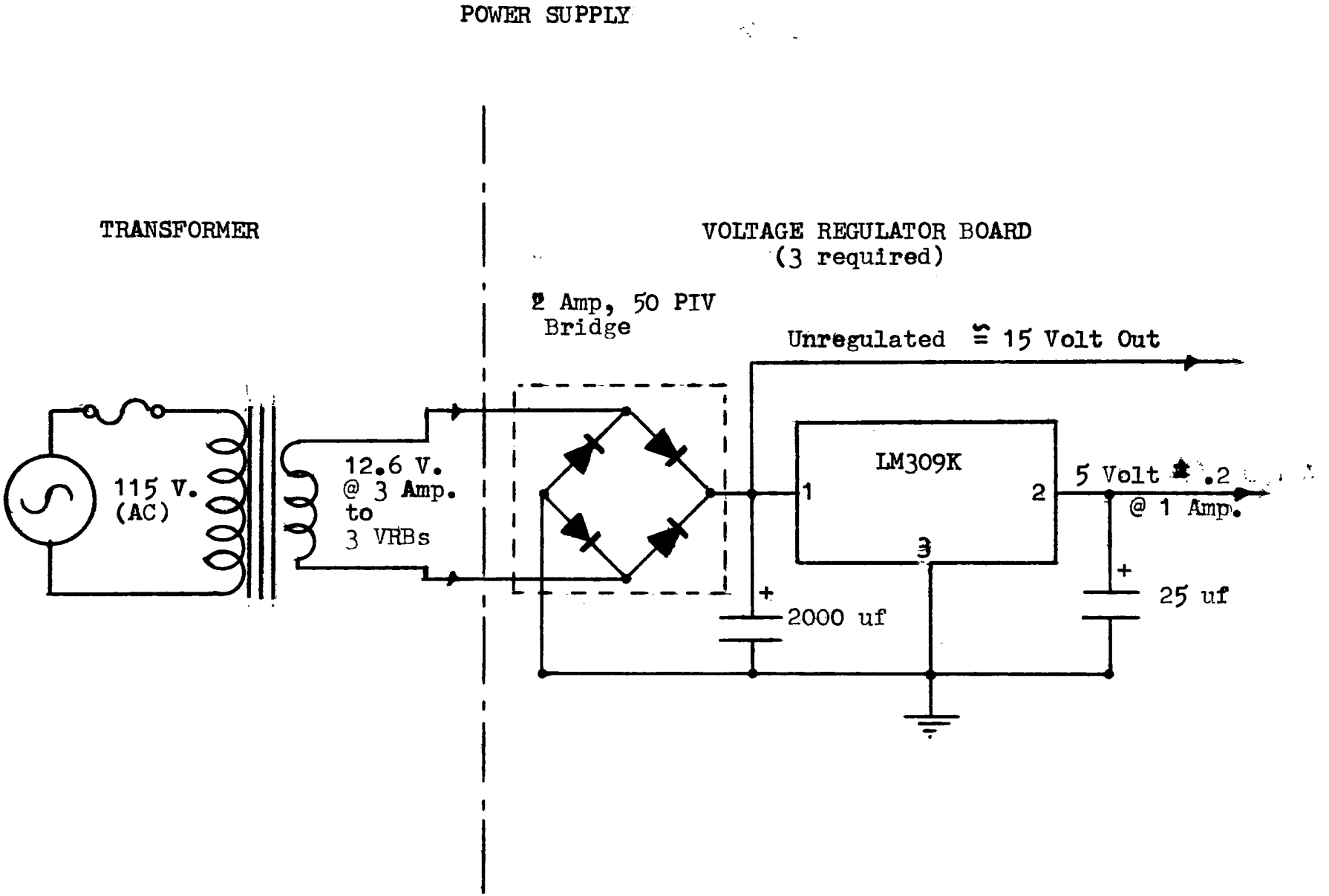
POWER SUPPLY
TRANSFORMER
VOLTAGE REGULATOR BOARD
(3 required)
2 Amp, 50 PIV
Bridge
Unregulated ≅ 15 Volt Out
115 V.
(AC)
12.6 V.
@ 3 Amp.
to
3 VRBs
LM309K
1
2
3
5 Volt ± .2
@ 1 Amp.
+
2000 uf
+
25 uf

Figure A-3

TIME BASE MODUAL

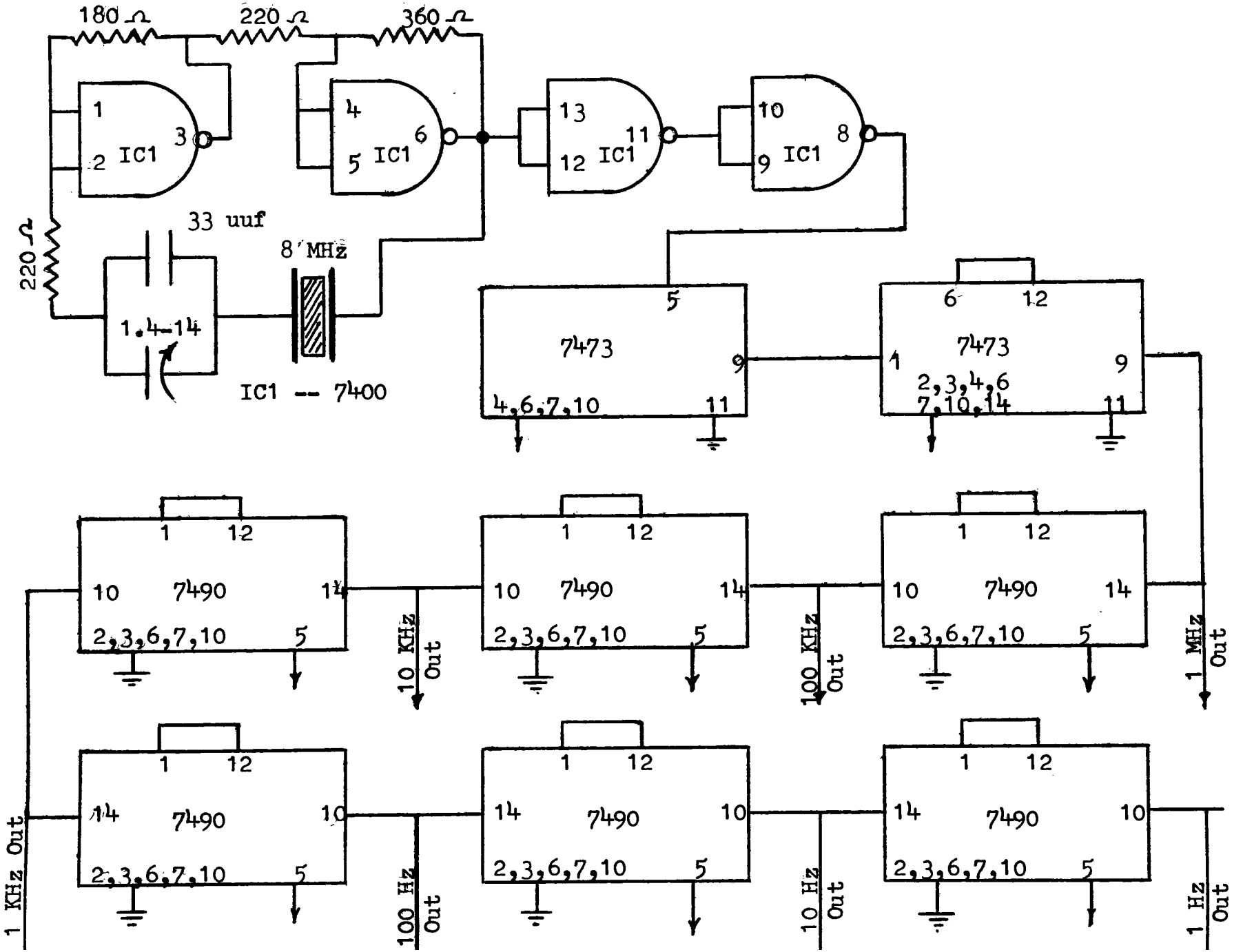

Figure A-4

BLOCK DIAGRAM TIMER

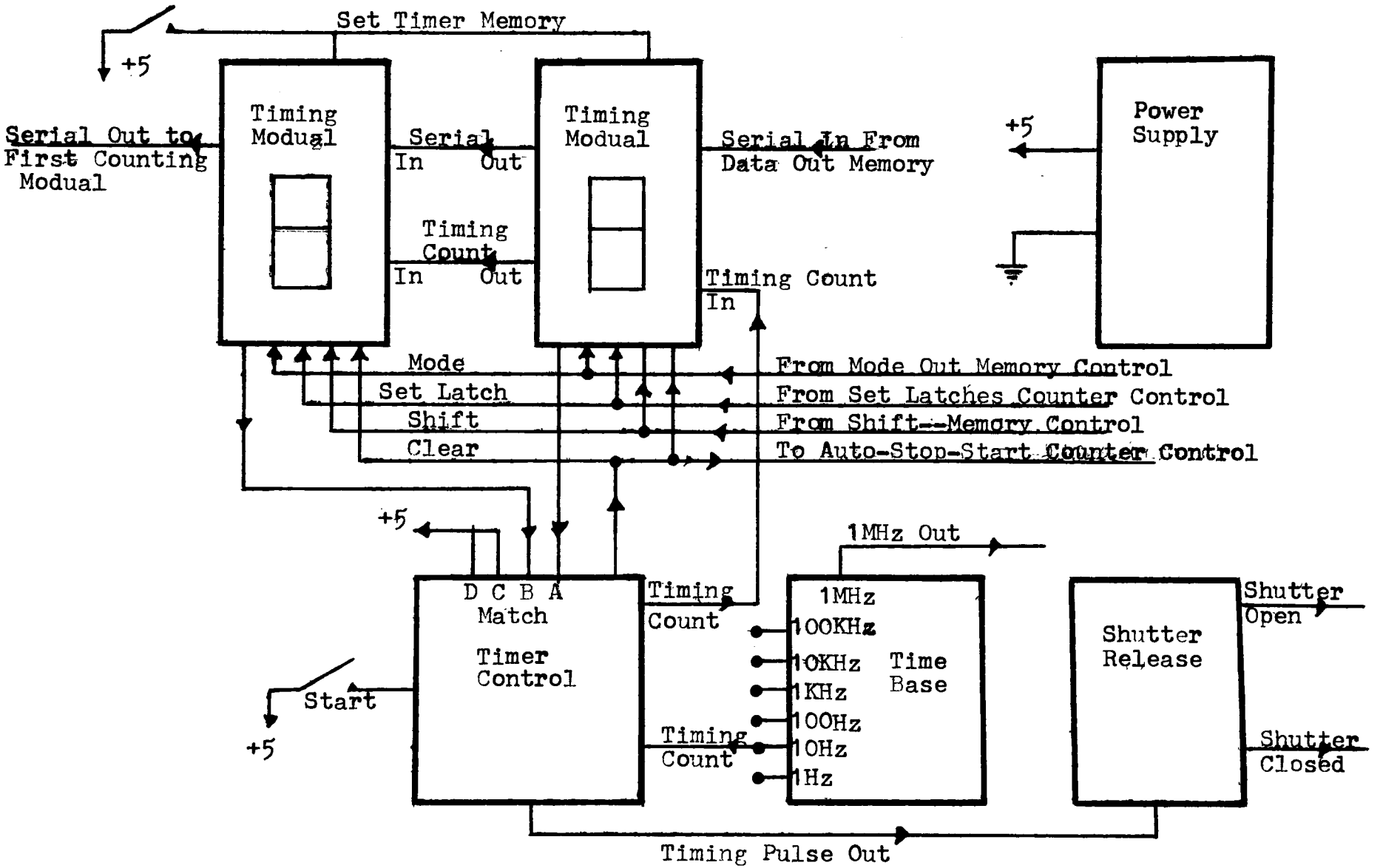

Figure A-5

TIMER COUNTER MODUAL

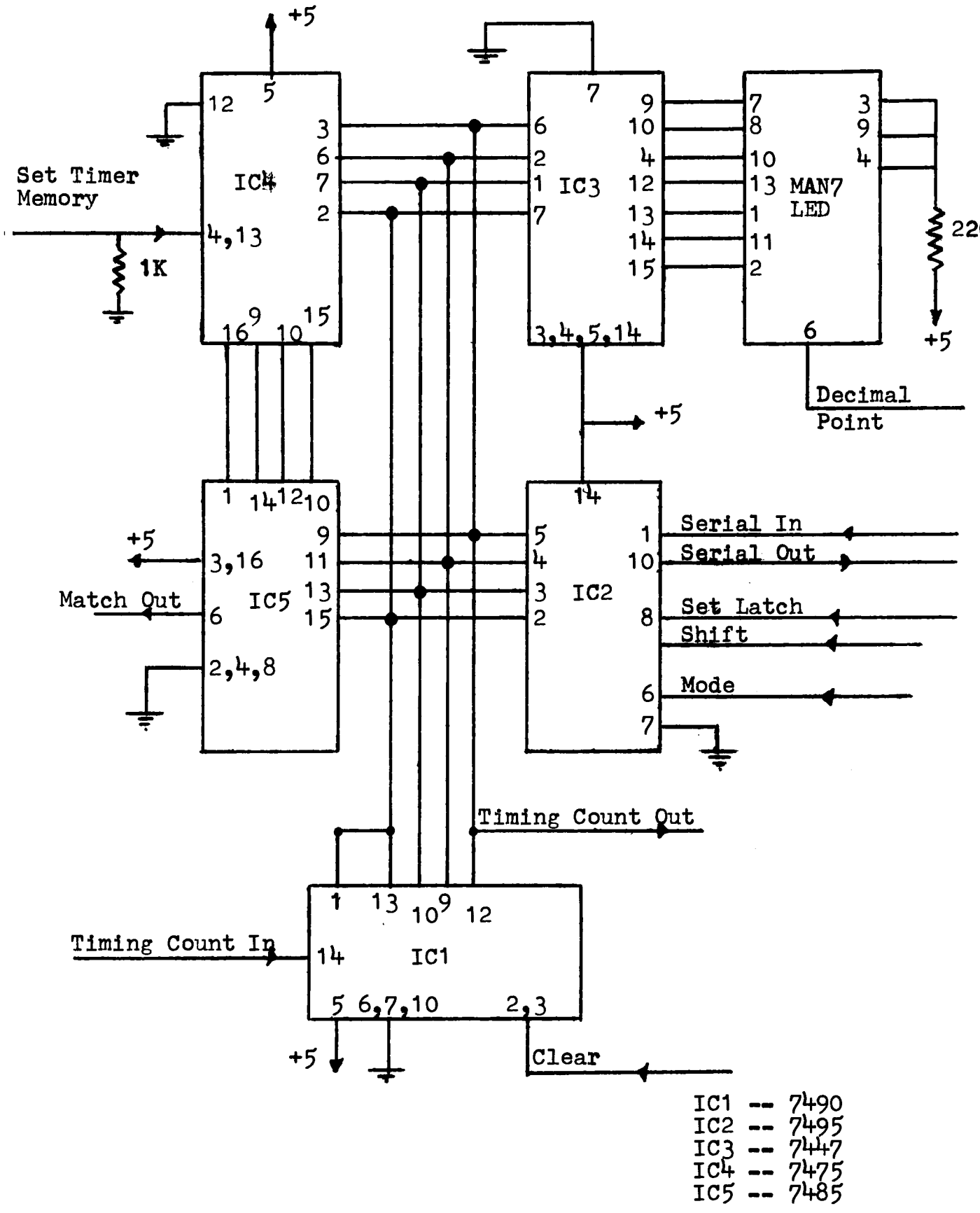

Figure A-6

TIMER CONTROL MODUAL

IC1 -- 7400
IC2 -- 7420
IC3 -- 7474
IC4 -- 74121

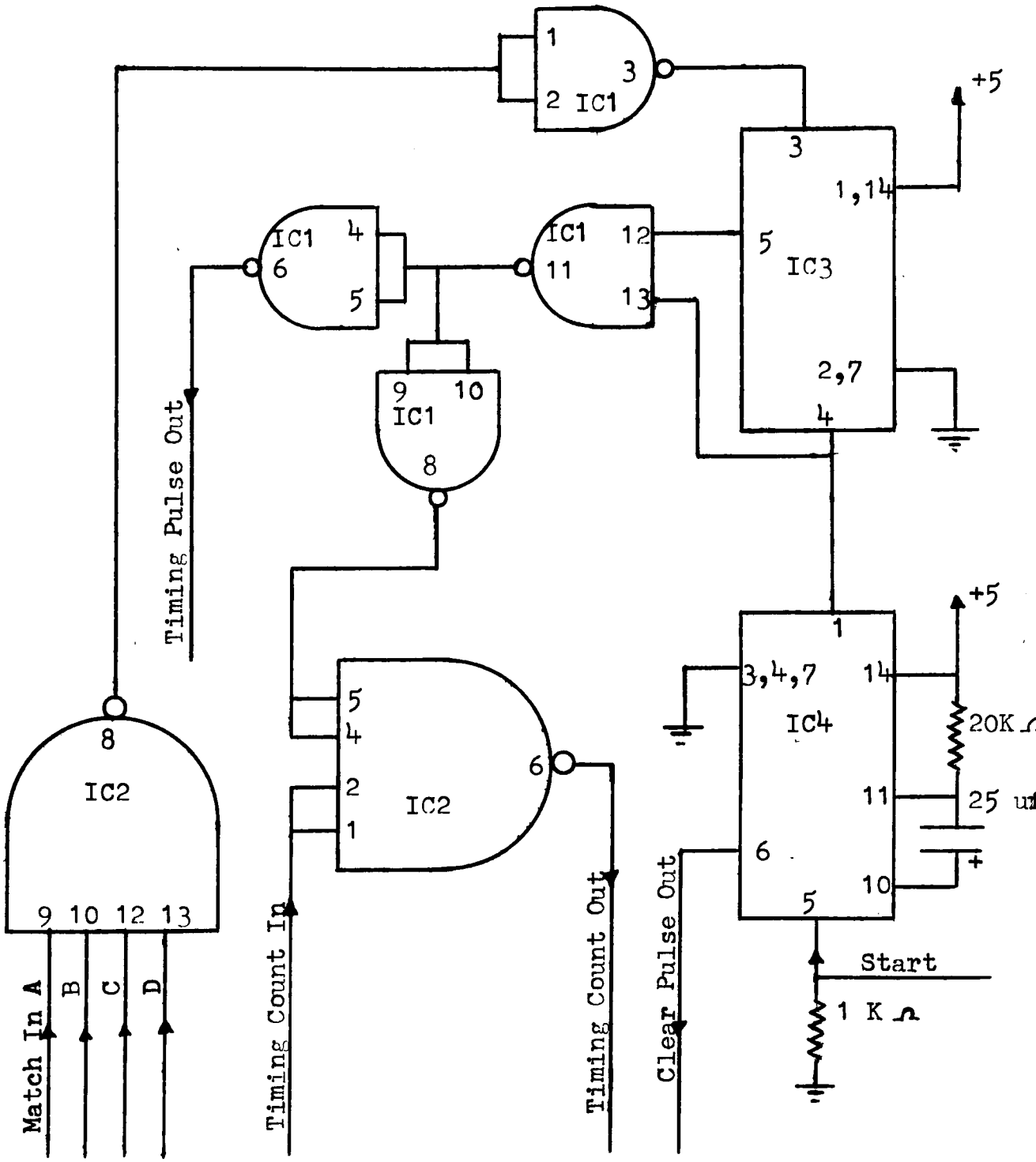

Figure A-7

SHUTTER RELEASE

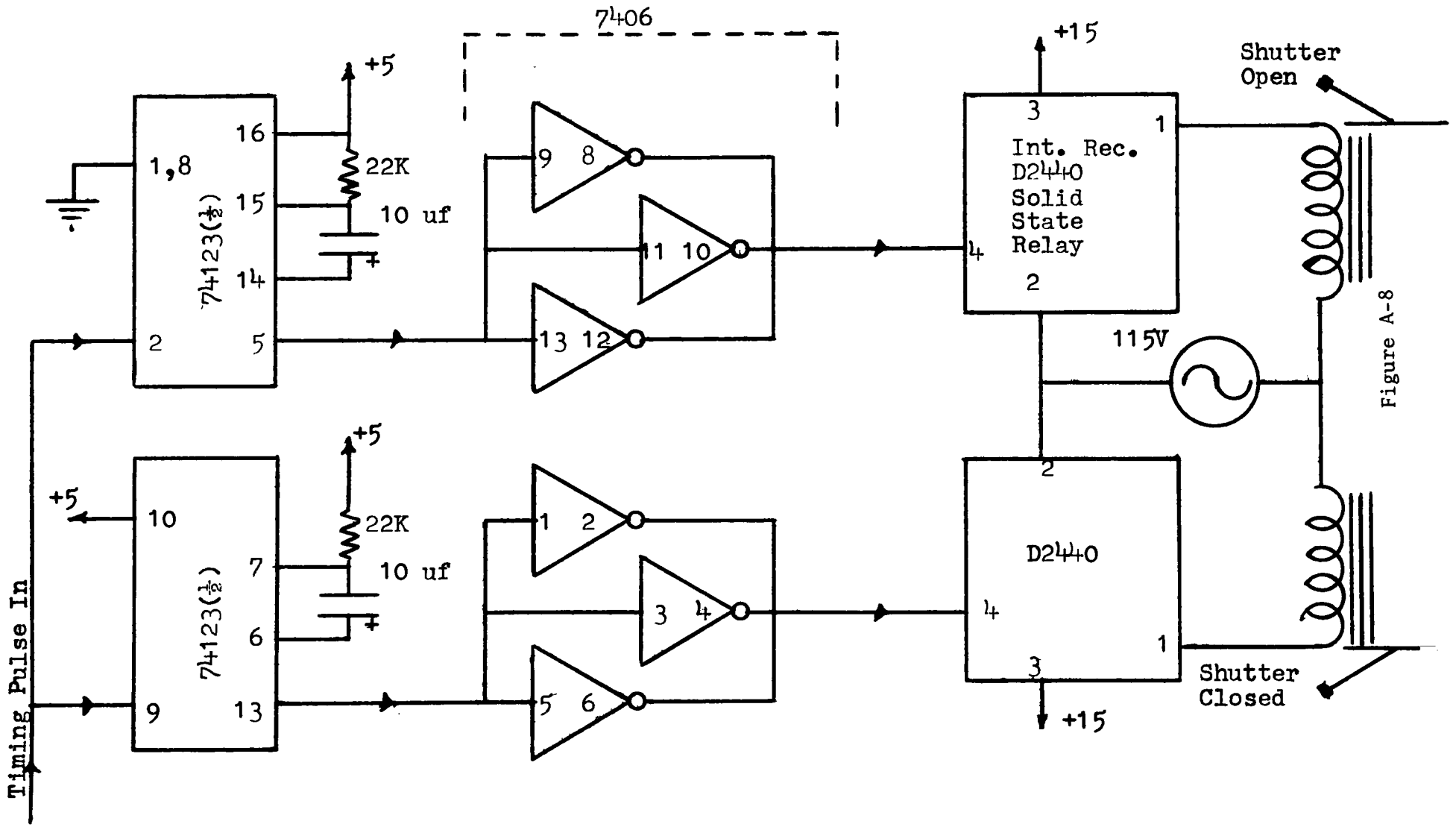

Figure A-8

BLOCK DIAGRAM COUNTER/MEMORY

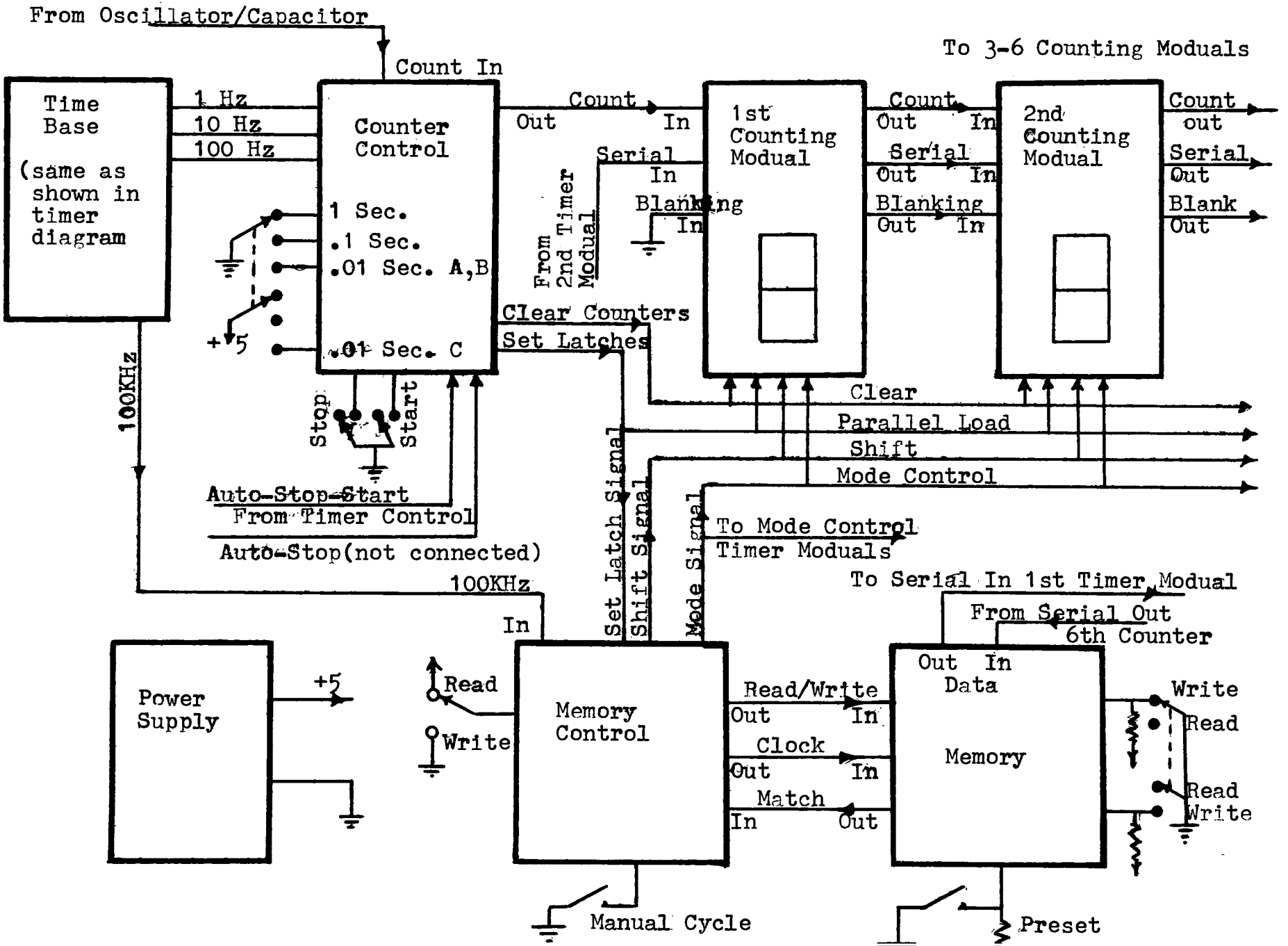

Figure A-9

COUNTER MODUAL

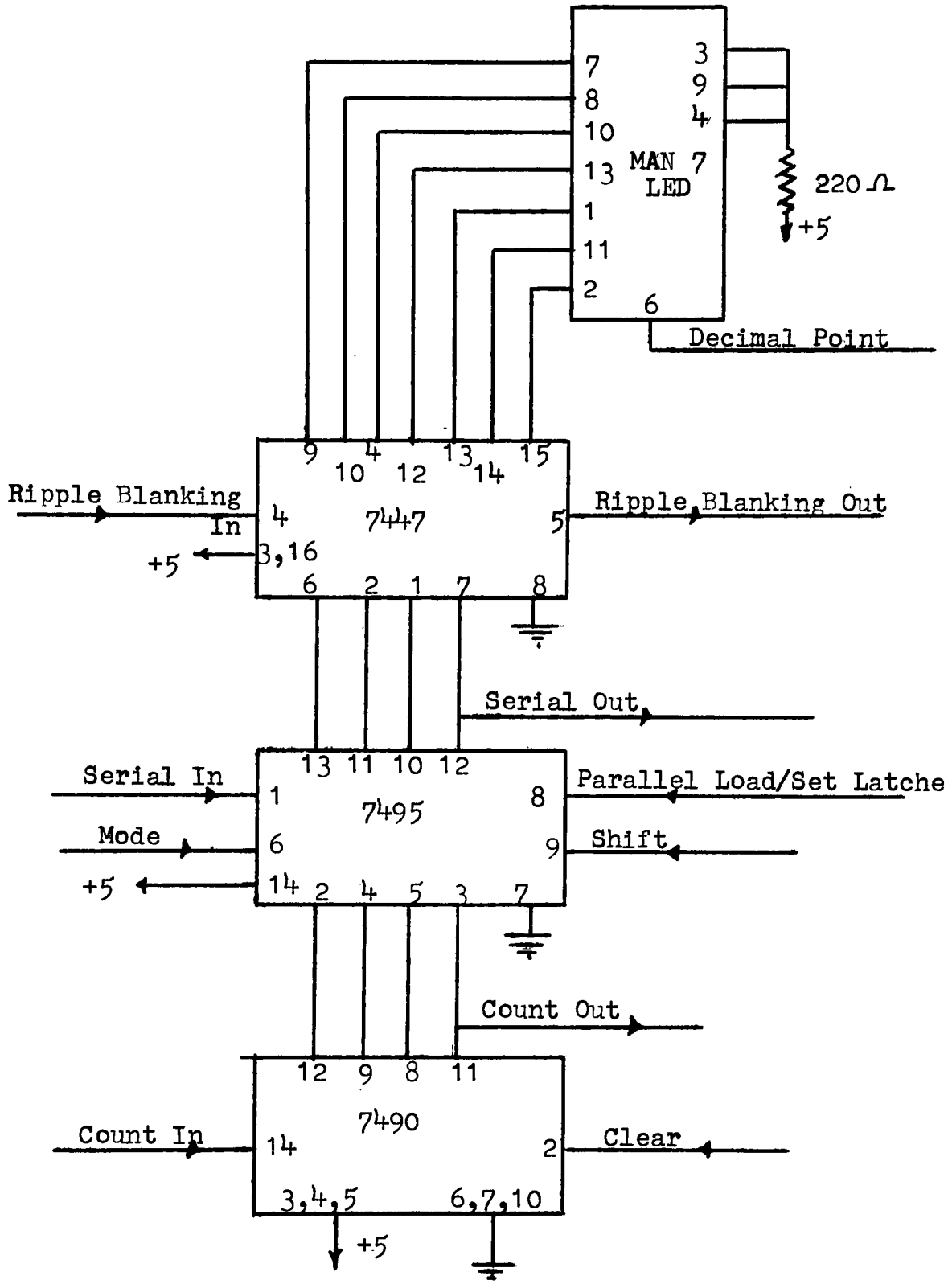

Figure A-10

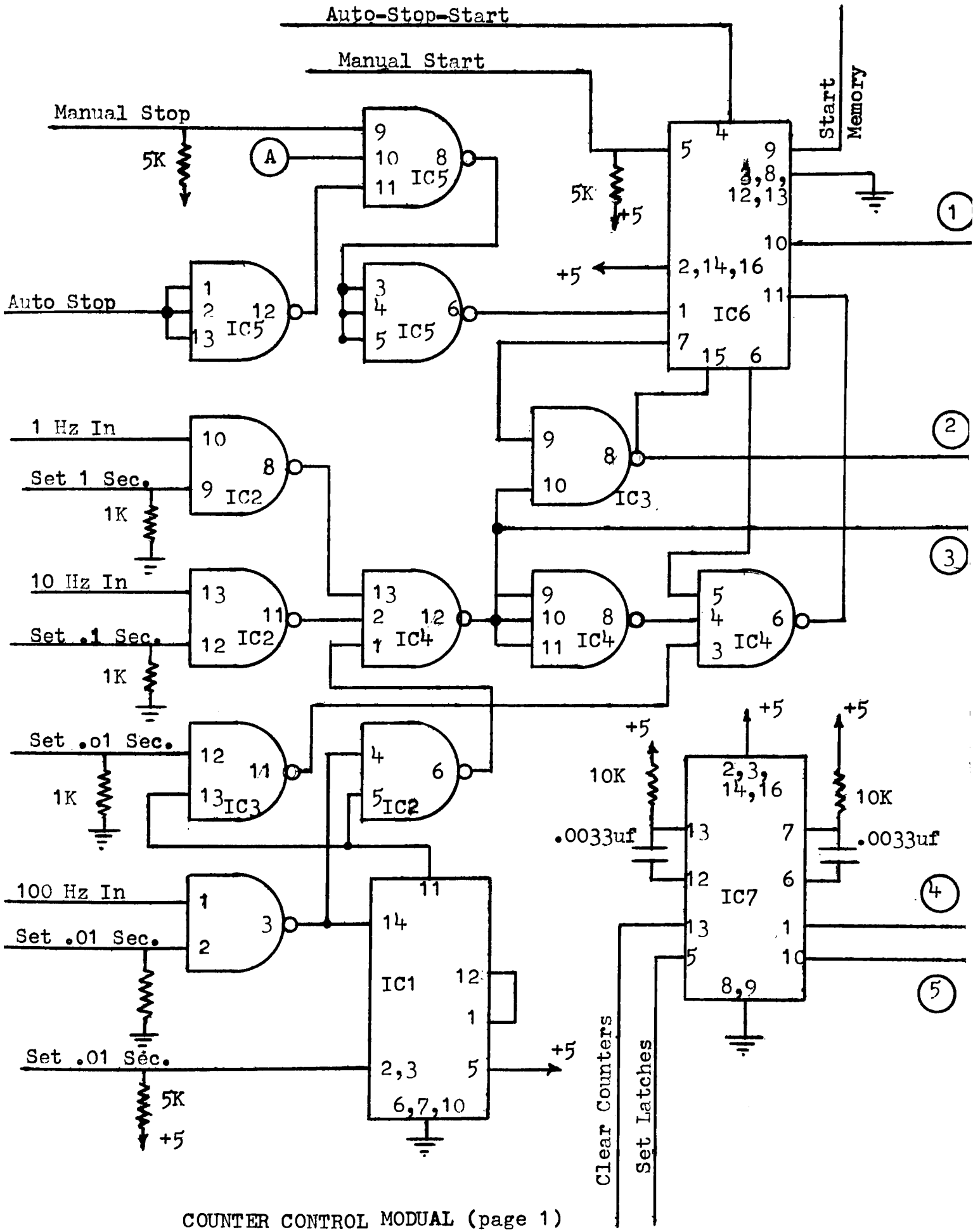

COUNTER CONTROL MODUAL (page 1)

Figure A-11a

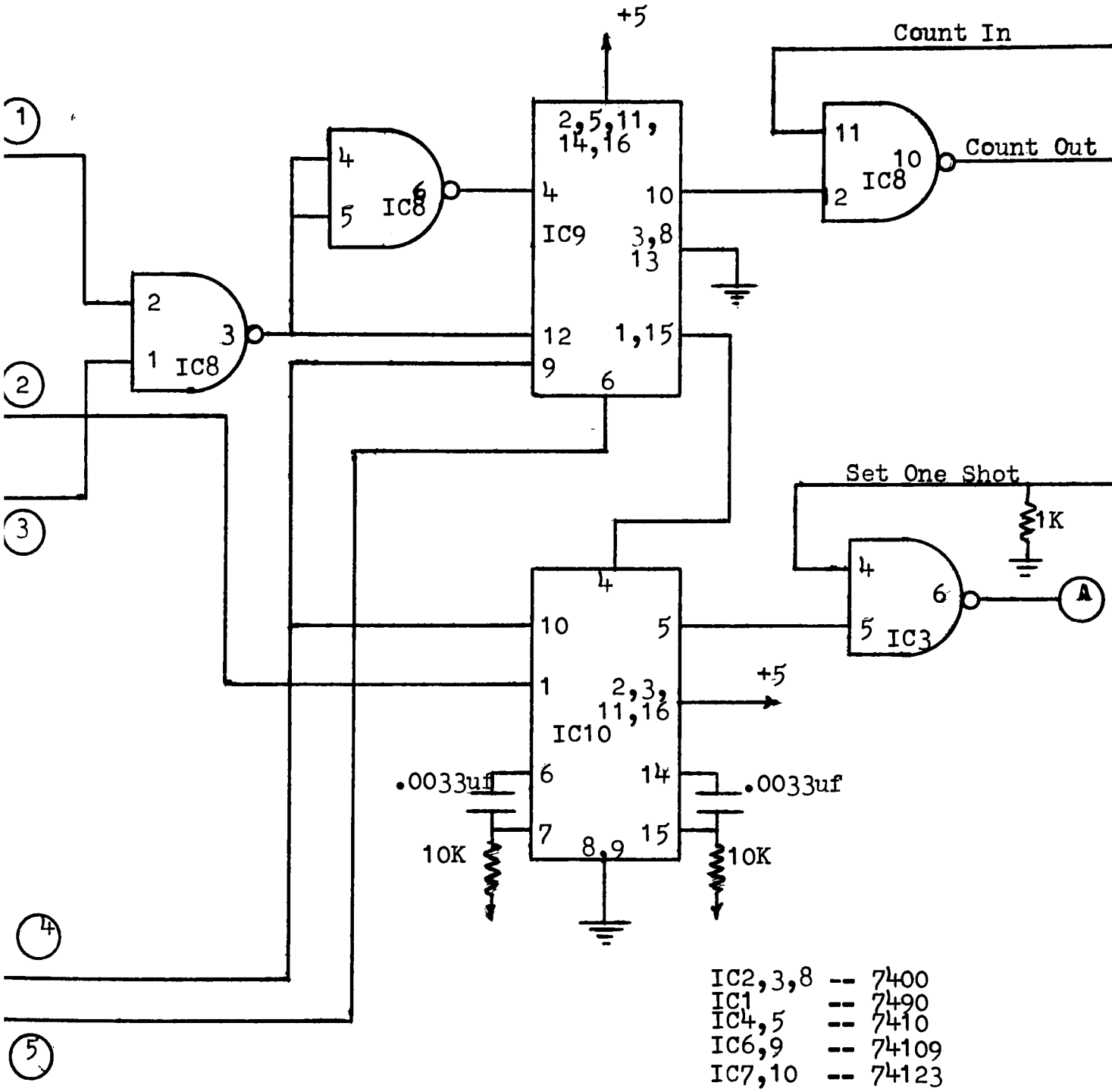

IC2,3,8 -- 7400
IC1 -- 7490
IC4,5 -- 7410
IC6,9 -- 74109
IC7,10 -- 74123

COUNTER CONTROL MODUAL (page 2)

Figure A-11b

MEMORY MODUAL

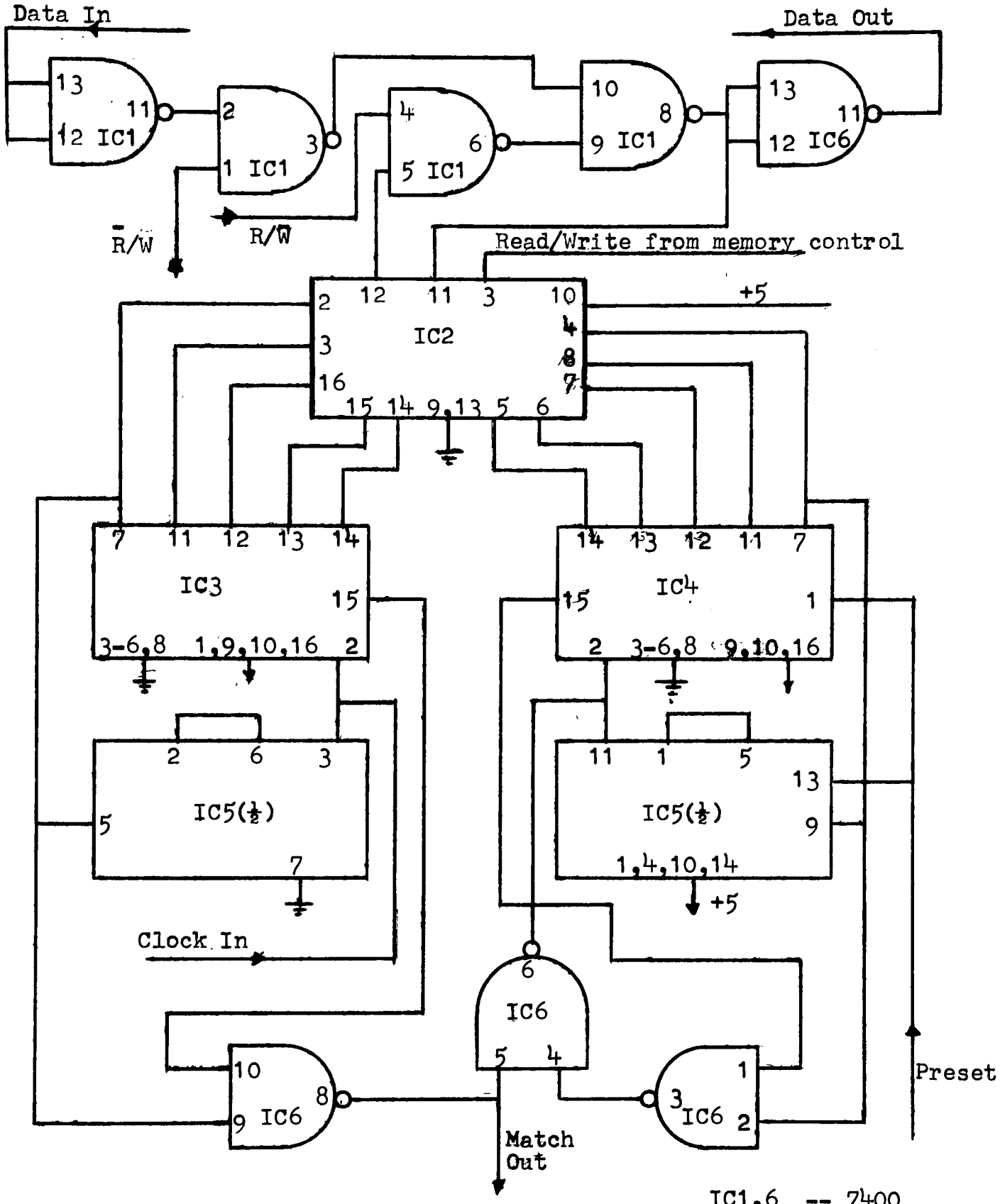

Figure A-12

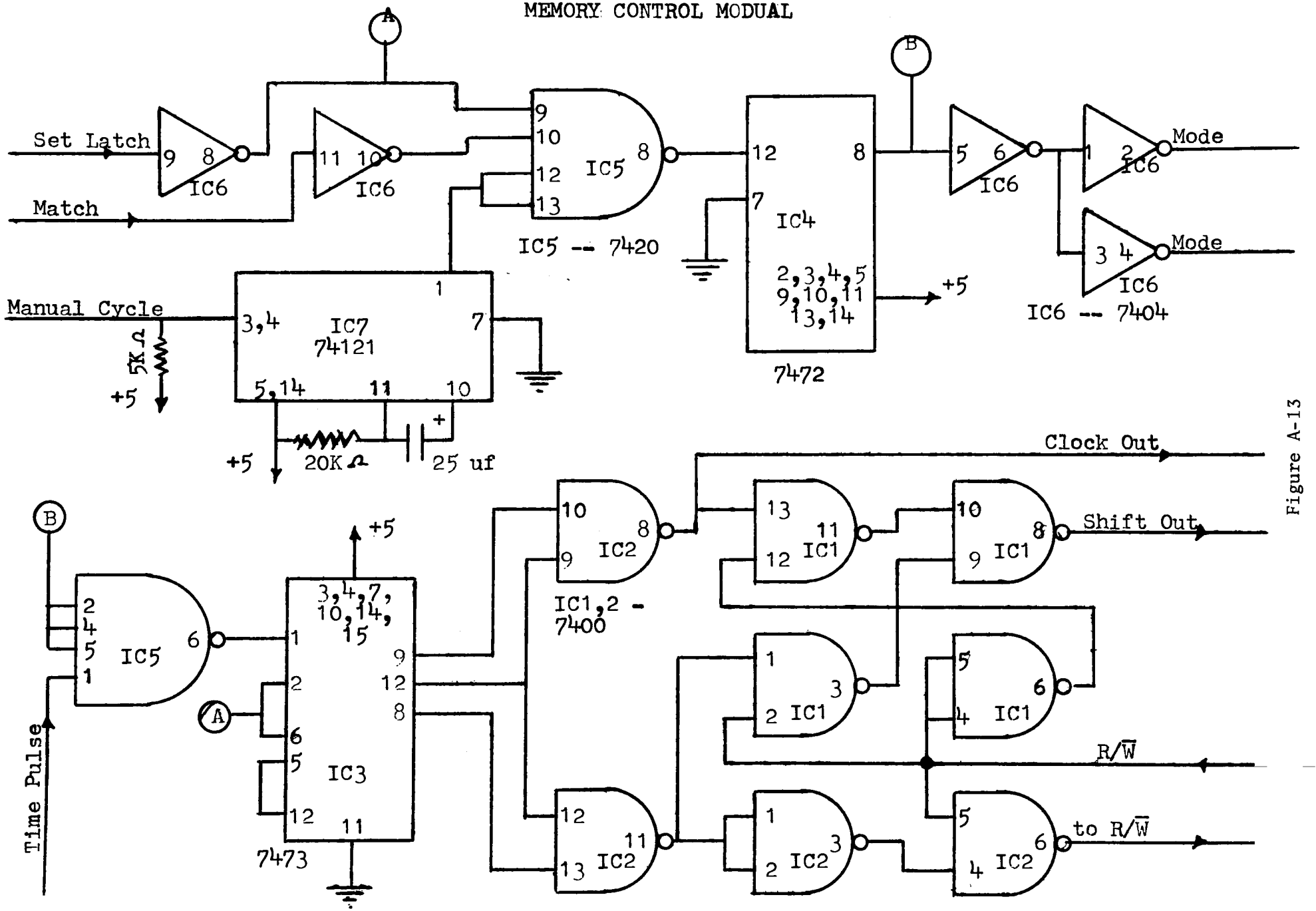
MEMORY CONTROL MODUAL
A
B
Set Latch
Match
IC6
IC6
IC5
IC5 -- 7420
IC4
2,3,4,5
9,10,11
13,14
7472
+5
IC6
IC6
Mode
Mode
IC6 -- 7404
Manual Cycle
IC7
74121
3,4
5,14
11
10
7
1
5K Ω
+5
20K Ω
25 uf
Clock Out
Shift Out
IC2
IC1
IC1,2 -
7400
IC5
IC3
3,4,7,
10,14,
15
7473
Time Pulse
R/W
to R/W
IC2
IC1
Figure A-13